Published for SISSA by Springer

Received: March 10, 2022
Accepted: May 19, 2022
Published: June 24, 2022

Gaudin models and multipoint conformal blocks III: comb channel coordinates and OPE factorisation

Ilija Burić,[a] **Sylvain Lacroix,**[b] **Jeremy Mann,**[c] **Lorenzo Quintavalle**[c] **and Volker Schomerus**[c,d,e]

[a] *Department of Physics, University of Pisa, Largo Pontecorvo 3, I-56127 Pisa, Italy*
[b] *Institute for Theoretical Studies, ETH Zürich, Clausiusstrasse 47, 8092 Zürich, Switzerland*
[c] *DESY Theory Group, DESY Hamburg, Notkestrasse 85, D-22603 Hamburg, Germany*
[d] *II. Institut für Theoretische Physik, Universität Hamburg, Luruper Chaussee 149, D-22761 Hamburg, Germany*
[e] *Zentrum für Mathematische Physik, Universität Hamburg, Bundesstrasse 55, D-20146 Hamburg, Germany*

E-mail: ilija.buric@df.unipi.it, sylvain.lacroix@eth-its.ethz.ch, jeremy.mann@desy.de, lorenzo.quintavalle@desy.de, volker.schomerus@desy.de

Abstract: We continue the exploration of multipoint scalar comb channel blocks for conformal field theories in 3D and 4D. The central goal here is to construct novel comb channel cross ratios that are well adapted to perform projections onto all intermediate primary fields. More concretely, our new set of cross ratios includes three for each intermediate mixed symmetry tensor exchange. These variables are designed such that the associated power series expansion coincides with the sum over descendants. The leading term of this expansion is argued to factorise into a product of lower point blocks. We establish this remarkable factorisation property by studying the limiting behaviour of the Gaudin Hamiltonians that are used to characterise multipoint conformal blocks. For six points we can map the eigenvalue equations for the limiting Gaudin differential operators to Casimir equations of spinning four-point blocks.

Keywords: Scale and Conformal Symmetries, Differential and Algebraic Geometry, Integrable Hierarchies

ArXiv ePrint: 2112.10827

https://doi.org/10.1007/JHEP06(2022)144

Contents

1 Introduction

During the last two decades, perturbative and non-perturbative aspects of conformal field theories have received widespread attention. Correlation functions of local operators are among the most important observables in these theories. These are complicated functions

JHEP06(2022)144

in general, in which the dynamical content of the theory is meshed together with the kinematics. In this context, conformal partial wave expansions allow us to disentangle the former frmo the latter. This makes them a central analytic tool of conformal field theory. Conformal partial waves, or the closely related conformal blocks, are entirely determined by conformal symmetry, i.e. they do not contain any dynamical information. When correlation functions are expanded in a basis of conformal blocks, the coefficients factorise into a product of three-point couplings. These are a set of numbers without any dependence on the insertion points of the fields, and they capture the whole dynamical content of the theory when combined with the spectrum of primaries.

In the case of four-point correlation functions, the relevant conformal blocks are by now well understood through the work of Dolan and Osborn and others, see in particular [1–14] and many further references therein. For correlation functions of N local fields with $N > 4$, similar powerful results on conformal blocks do not yet exist, though there is some significant recent activity in this area, see for example [15–30]. For this reason, we initiated a novel, integrability based approach to multipoint conformal blocks in [26]. It extends an idea that was advanced initially by Dolan and Osborn, namely to characterise conformal blocks through the set of differential equations that they satisfy. For four-point blocks, these differential equations are eigenvalue equations for the set of commuting Casimir differential operators that measure the conformal weight and spin of the intermediate field. For a higher number N of insertion points, the operators that measure the quantum numbers of the $N-3$ intermediate fields are still mutually commuting, but they do not suffice to characterise the associated blocks. The challenge to complete the Casimir-like operators into a full set of commuting differential operators was solved in [26, 29]. In these papers we explained how to obtain the missing differential operators by taking limits of an N-site Gaudin integrable system [31–33].

The set of differential equations and blocks depend on the choice of an OPE channel. Among all possible channels, the so-called comb and snowflake for an $N = 6$ point function have received the most attention so far. A detailed discussion of all possible channel topologies and their corresponding Gaudin limits can be found in part I of this series [29]. In part II, we then went on to study what we call vertex systems, i.e. three-point blocks for spinning fields. In the case of three-point functions of one scalar and up to two mixed symmetry tensors (MSTs) in $d \leq 4$, we were able to identify the unique Gaudin differential operator of this system. This covers all comb channel vertices that can appear in $d = 3$ and $d = 4$ dimensions. In the case where the two spinning fields in the three-point function are symmetric traceless tensors (STTs), we were able to show that the three-point vertex operator is included in the set of five differential operators that characterise a five-point function. This was achieved by performing appropriate OPE limits to reduce the five-point to a three-point function. At the time, the extension of this analysis to comb channel N-point blocks with vertices including MSTs was hampered by the absence of cross ratios compatible with the relevant limits. This is one of the motivations for part III of our series. We will manage to construct a set of cross ratios for N-point functions in the comb channel that is perfectly adapted to OPE factorisations into lower point blocks. The explicit formulas are developed for $d \leq 4$ dimensions, but the ideas are more general and should admit an extension to higher d.

JHEP06(2022)144

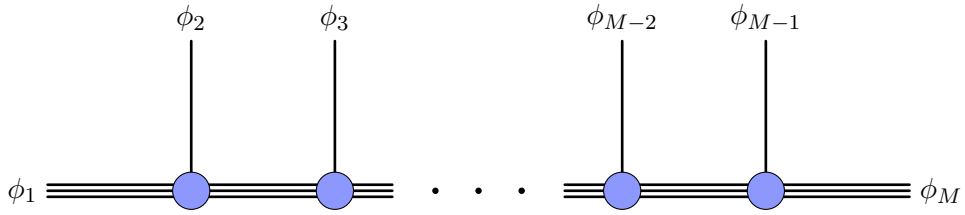

Figure 1: Schematic representation of an M-point comb channel OPE diagram in $d = 4$. All the external legs at the interior of the comb are scalars, while we allow fields ϕ_1 and ϕ_M to sit in a generic representation.

Let us now describe the main new results of this work in some detail. To set up some notation, we consider the comb channel for M fields in $d = 4$, see figure 1.[1] In general, we can insert arbitrary spinning fields at the external legs, but we shall assume that the fields ϕ_j on the external legs $j = 2, \ldots, M-1$ in the interior of the comb are scalar fields of conformal weight Δ_j. The two fields ϕ_1 and ϕ_M at the two sides of the comb are allowed to carry any spin, i.e. they can be symmetric traceless tensors (STTs) or even mixed symmetry tensors (MSTs). We denote the quantum numbers of these fields by $\varphi_1 = [\Delta_L, l_L, \ell_L]$ and $\varphi_M = [\Delta_R, l_R, \ell_R]$. Here, the subscripts L and R stand for 'left' and 'right', respectively, in accordance with their position in the OPE diagram. Note that STTs correspond to fields with $\ell = 0$ and scalar fields are obtained if we also set $l = 0$. The intermediate fields that appear along the horizontal lines of the comb are labeled by $[s]$ with $s = 1, \ldots, M-3$. We may think of $[s] = \{s+1, s+2\}$ as a pair of consecutive integers that enumerate the two external scalar fields attached to the two sides of the internal link. The associated intermediate fields $\Phi_{[s]}$ possess quantum numbers $\varphi_{[s]} = [\Delta_s, l_s, \ell_s]$ with non-vanishing ℓ_s in generic cases. Only ϕ_1 being scalar enforces $\ell_1 = 0$ at the first internal leg, and similarly $\ell_{M-3} = 0$ in case ϕ_M is scalar. When $M > 4$, the total number of cross ratios for M-point functions with $M-2$ scalar and two spinning insertions is given by

$$n_{cr}^{M} = 4(M-3) + 1 - 2\delta_{l_L=0=\ell_L} - 2\delta_{l_R=0=\ell_R}\,. \tag{1.1}$$

The subtractions correspond to the cases in which either one or both of the fields ϕ_1, ϕ_M are scalar. An $M = 3$-point function (vertex) with one scalar external field has no cross ratios unless the other two fields are both spinning, in which case there is a unique cross ratio, see [34]. For $M = 4$ points with at least two scalar insertions, one has

$$n_{cr}^{M=4} = 5 - 2\delta_{l_L=0=\ell_L} - 2\delta_{l_R=0=\ell_R} + \delta_{l_L=0=\ell_L}\delta_{l_R=0=\ell_R}\,. \tag{1.2}$$

Note that the application to a four-point function of four scalar fields gives $n_{cr}^{M=4} = 5 - 4 + 1 = 2$, i.e. there are two cross ratios in this case, as is well known.

The comb channel Hamiltonians are relatively easy to construct, at least in principle. In order to do so, we employ the first order differential operators $\mathcal{T}_{j,\alpha}, j = 1, \ldots M$, that

[1] The following discussion is later applied to subdiagrams of an N-point comb channel OPE diagram, which is why we do not set $M = N$ and also allow for two of the external fields to carry spin.

JHEP06(2022)144

correspond to the action of the conformal generators T_a on primary fields $\phi_j(x_j)$. In addition, let us also define

$$\mathcal{T}_{[s],\alpha} = \sum_{k=1}^{s+1} \mathcal{T}_{k,\alpha}\,. \tag{1.3}$$

The Casimir differential operators $\mathcal{D}^s_p, s = 1, \ldots, M-3$, are given by the p^{th}-order Casimir element for the generators $\mathcal{T}_{[s],\alpha}$. For generic comb channel links in $d = 4$, the integer p assumes the values $p = 2, 3, 4$. In cases where the field ϕ_1 is a scalar, the first link only carries two quantum numbers. There must hence be one relation between the three Casimir elements, such that one can restrict to $p = 2, 4$. A similar statement holds when the field ϕ_M is scalar. In addition, we have fourth order vertex differential operators of the form

$$\mathcal{V}^4_s = \kappa_4^{\alpha_1\ldots\alpha_4} \mathcal{S}_{s,\alpha_1} \cdots \mathcal{S}_{s,\alpha_4}, \qquad \mathcal{S}_{s,\alpha} = \mathcal{T}_{s+1,\alpha} - \mathcal{T}_{[s-1],\alpha} \tag{1.4}$$

for $s = 1, \ldots, M-2$. The operators $\mathcal{V}^4_1$ and $\mathcal{V}^4_{M-2}$ can be expressed in terms of the Casimir differential operators whenever ϕ_1 and ϕ_M are both scalar. So the number of differential operators we have constructed here coincides with the number n^M_{cr} of cross ratios. As we have shown in [29], these operators are all independent and they are mutually commuting. Let us note that the set of operators satisfying these properties is of course not unique. In our discussion of the six-point function, we will work with a set that is slightly different from the one we described here.

The joint eigenfunctions of these operators depend on the weights $\Delta_j, j = 2, \ldots, M-1$ of the external scalar fields, as well as the quantum numbers $\varphi_1 = [\Delta_L, l_L, \ell_L]$ and $\varphi_M = [\Delta_R, l_R, \ell_R]$ of the two fields ϕ_1 and ϕ_M, respectively. Of course, they also depend on the eigenvalues of the differential operators. We parameterise the eigenvalues of the Casimir differential operators through the quantum numbers $\varphi_{[s]} = [\Delta_s, l_s, \ell_s], s = 1, \ldots, M-3$ of the internal primaries, and we define $\tau_s, s = 1, \ldots, M-2$, to be the eigenvalues of the vertex differential operators $\mathcal{V}^s_4$. The latter correspond to a choice of tensor structures at the vertices. These wave functions are denoted by

$$\Psi^{\varphi_1,\Delta_j,\varphi_M}_{[\Delta_s,l_s,\ell_s;\tau_s]} = \Psi^{\varphi_1,\Delta_j,\varphi_M}_{[\Delta_s,l_s,\ell_s;\tau_s]}(u) \tag{1.5}$$

where u denotes any set of n^M_{cr} independent cross ratios. While the construction of the n_{cr} differential equations that these functions satisfy is fully algorithmic, see previous paragraph, the resulting expressions are rather lengthy in general, see e.g. [29] for some examples. Nevertheless, there are a few cases for which one obtains well-known differential operators. For $M = 3$ with two spinning fields ϕ_1, ϕ_3, the unique vertex differential operator was shown in [34] to coincide with the lemniscatic elliptic Calogero-Moser-Sutherland Hamiltonian discovered by Etingof, Felder, Ma and Veselov in [35]. The most well-known system appears for $M = 4$ when all the fields ϕ_i are scalar. In this case the resulting Hamiltonians famously coincide with those of a 2-particle hyperbolic Calogero-Sutherland model of type BC_2, [36]. The associated eigenvalue equations turn out to be equivalent to the Casimir equations for scalar four-point blocks that were calculated and analysed by Dolan and Osborn [2]. The corresponding eigenfunctions have been studied extensively. In

JHEP06(2022)144

mathematics, this was initiated by the work of Heckman and Opdam [37]. The most relevant mathematical results were later re-derived independently in physics, starting with the work of Dolan and Osborn [1–3]. Continuing with $M = 4$, the next step is to include cases in which one or both of the fields ϕ_1 and ϕ_4 carry spin. Systems of this type have been studied in the physics literature by [4, 9, 38]. In particular, so-called seed conformal blocks in $d = 4$ dimensions have been characterised through a set of Casimir differential equations. The solution for these special blocks was developed in the same papers, and extensions to more general blocks in [12]. Alternatively, it is also possible to derive Casimir differential equations within the context of harmonic analysis of the conformal group [39–41]. In this context, the generalization to a universal spinning 2-particle Calogero-Sutherland Hamiltonian for any choice of spin representations of ϕ_1 and ϕ_4 can be constructed from Harish-Chandra's radial component map [42], as will be discussed in [43]. The radial component map provides Casimir equations for spinning four-point blocks with external fields of arbitrary spin and in any dimension, thereby vastly generalising its current status in the physics literature. In spite of being so general, the resulting expressions for the universal spinning Casimir operators turn out to be surprisingly compact. Nevertheless, a universal solution theory has not yet been developed.

After this preparation we are now able to state the main results of this work. They concern conformal blocks for correlation functions of N scalar fields. Obviously, the explicit form of the differential operators depends very much on the coordinates/cross ratios that are being used. Below, we shall start with one relatively simple choice that consists of $2(N-3)$ four-point cross ratios, $N-4$ five-point cross ratios and $N-5$ six-point cross ratios. The total number is $4N-15$ which coincides with the number of cross ratios of a scalar N-point function in $d = 4$ when $N > 4$. These initial cross ratios are depicted in figures 2a and 3. They turn out to be well adapted to performing explicit computations. In particular, one can verify that all the coefficients of the differential operators are polynomials in these cross ratios. For this reason we shall refer to them as 'polynomial' cross ratios.

The key to this work is contained in subsection 2.4, where we introduce a new set of independent conformal invariants, first for $N = 6$ and then more generally for any number N of insertions. The $2(N-3)$ four-point cross ratios mentioned above give rise to $N-3$ pairs $(z_r, \bar{z}_r), r = 1, \ldots, N-3$, of invariants, one for each internal edge. These are direct generalisations of the usual invariants $z, \bar{z}$ that are used to parameterise four-point cross ratios. The five-point cross ratios are then employed to build $N-4$ invariants $w_r, r = 2, \ldots, N-3$, one for each non-trivial vertex. The construction of the w_r is an immediate extension of the variable w that we introduced in the study of five-point blocks in our previous work [29], to complement the variables $z_1, \bar{z}_1, z_2, \bar{z}_2$. But starting with $N = 6$, there exists $N-5$ additional independent invariants that involve the six-point cross ratios we described above. From these we define new conformal invariants $\Upsilon_r, r = 2, \ldots, N-4$, one for each internal edge in which an MST can propagate. This invariant is first constructed for the unique intermediate MST exchange in a six-point comb channel diagram for scalar external fields, see eq. (2.24), and then extended to higher numbers $N \geq 6$ of insertions at the end of section 2.4. In the same subsection, we also provide a nice geometrical interpretation of the new conformal invariants, which we shall refer to as comb channel OPE coordinates.

JHEP06(2022)144

The association of these invariants with specific links and vertices is much more than mere counting. Consider a link $r \in \{2, \ldots, N-4\}$ in which an MST propagates. This link comes with a set of three invariants $z_r, \bar{z}_r, \Upsilon_r$. Our central claim concerning OPE factorisation of multipoint blocks can now be formulated after rewriting the blocks Ψ in terms of the OPE coordinates $\Psi = \Psi(z_r, \bar{z}_r, \Upsilon_r; w_s)$. When these functions are expanded around $z_b = \bar{z}_b = 0 = \Upsilon_b$,[2] for one particular value of $b \in \{2, \ldots, N-4\}$ the leading term is claimed to be of the form

$$\begin{aligned}\Psi^{\Delta_i}_{[\Delta_r, l_r, \ell_r; \tau_r]}(z_r, \bar{z}_r, \Upsilon_r; w_s) = z_b^{\frac{1}{2}(\Delta_b + l_b + \ell_b)} \bar{z}_b^{\frac{1}{2}(\Delta_b - l_b - \ell_b)} \Upsilon_b^{\ell_b} \times \\ \times \Bigg(\Psi^{\Delta_{i \leq b+1}, [\Delta_b, l_b, \ell_b]}_{[\Delta_r, l_r, \ell_r; \tau_s]} (z_r, \bar{z}_r, \Upsilon_r; w_s)^{r<b}_{s<b} \\ \times \Psi^{[\Delta_b, l_b, \ell_b], \Delta_{i>b+1}}_{[\Delta_r, l_r, \ell_r; \tau_s]} (z_r, \bar{z}_r, \Upsilon_r; w_s)^{r>b}_{s \geq b} + O(z_b, \bar{z}_b, \Upsilon_b) \Bigg) .\end{aligned} \tag{1.6}$$

In the first line we have displayed the leading exponents in any of the three variables. Note that these are determined by the quantum numbers of the exchanged intermediate field $\phi_{[b]}$. In case the latter is an STT, that is if and only if $\ell_b = 0$, this leading term is familiar from the theory of blocks for four-point functions of scalars. Once this term in the first line of the expression is factored out, the remaining function admits a power series expansion in the three variables $z_b, \bar{z}_b$ and Υ_b. The constant term in this power series expansion turns out to factorise into a product of two eigenfunctions of Gaudin Hamiltonians with $M_1 = b + 2$ and $M_2 = N - b$ sites, respectively. The sub- and superscripts we have placed on the eigenfunctions restrict the dependence on both the quantum numbers and the conformal invariants. Let us note that this OPE factorisation also holds for $b = 1$ and $b = N - 3$, except that in these two cases, the prefactor in the first line only contains powers of z_b and $\bar{z}_b$ because $\ell_b = 0$. In both such cases, one of the two blocks in the second line is simply a constant. One can directly verify such factorisation formulas whenever explicit formulas for the blocks are available, e.g. for $d = 1$ comb-channel blocks, which have been constructed in [15]. We have included one such explicit check for the six-point function in appendix D.

To prove the remarkable result (1.6) beyond those cases in which the blocks are known, the differential operators play a decisive role. Strictly speaking, our central claim remains conjectural for $N > 6$. But in the case of $N = 6$ we are able to establish it rigorously. A scalar six-point function in $d = 4$ dimensions depends on nine cross ratios. We parameterise these through the variables $z_r, \bar{z}_r, r = 1, 2, 3$, $\Upsilon = \Upsilon_2$ and $w_s, s = 1, 2$. When we perform the limit on the variables $(z_2, \bar{z}_2, \Upsilon)$ that are associated with the internal MST exchange along the central link, the block factorises into a product of two spinning $M = 4$-point blocks with a single spinning field and three scalars in each of them. Such spinning four-point blocks depend on three variables each. In our special parameterisation, these are given by $(z_1, \bar{z}_1; w_1)$ and $(z_3, \bar{z}_3; w_2)$, respectively. As we recalled above, spinning four-point

[2] Note that the three limits do not commute. We take the limit $\bar{z}_b \to 0$ first before taking z_b and Υ_b to zero. For these last two variables the order of limits does not matter.

JHEP06(2022)144

blocks may be characterised as solutions of a specific set of differential equations that has been worked out at least for some examples in the CFT literature, see in particular [9]. As we will announce in this paper, the full set of these differential equations can been obtained with the help of Harish-Chandra's radial component map [43]. The strategy to prove our factorisation result is to evaluate the limit of the six-site Gaudin Hamiltonians as $z_2, \bar{z}_2, \Upsilon$ are sent to zero and to map the resulting operators to the differential operators for spinning four-point blocks through an appropriate change of variables. Similarly, one can also consider the limit in which the pairs $(z_1, \bar{z}_1)$ and $(z_3, \bar{z}_3)$ are both sent to zero. Our OPE factorisation states that the leading term in the resulting expansion is given by a spinning four-point block for two scalar and two spinning fields. Once again, it is possible to verify this claim by mapping the relevant differential operators onto each other.

Let us now briefly outline the content of each section. The next section is entirely devoted to a discussion of cross ratios. After a brief review of the two most commonly used sets of cross ratios for four-point functions, we will extend both of them to multipoint functions. The usual cross ratios u, v can be generalised to higher numbers N of insertion points in such a way that the Casimir differential operators for comb channel blocks have polynomial coefficients, at least for $N \leq 10$. These *polynomial cross ratios* for multipoint functions are defined in section 2.2. While the latter have some nice features, they are not well adapted to taking OPE limits. For this reason we shall introduce a second set of conformal invariants which we dub *OPE cross ratios*. We do so for $N = 5$ and $N = 6$ points first before discussing the case $N > 6$, based on a geometric/group theoretic interpretation of these variables. Section 3 is devoted to OPE limits, and the discussion focuses on $N = 6$-point functions. After a brief review of the Gaudin Hamiltonians that characterise comb channel blocks, we derive the asymptotic behaviour in the first line of eq. (1.6) and show that the leading term indeed factorises into a product of functions of the respective variables. These functions may be characterised through certain differential operators which can be obtained by studying the limiting behaviour of the original Gaudin Hamiltonians. In particular, it turns out that the Gaudin Hamiltonians split into two sets of operators that act on a disjoint subset of cross ratios. In section 4, we will identify these limiting differential operators with the Casimir operators of spinning four-point blocks. To this end, we briefly sketch the results of [43] on the universal spinning Casimir operators. We cast these results in the form of universal spinning Calogero-Sutherland Hamiltonians before we compare these operators with those obtained in section 3 by taking the OPE limit of multipoint functions. It turns out that the two sets of operators coincide. This establishes our result (1.6), including the identification of the leading term with a product of lower point conformal blocks. The text concludes with a brief summary, along with a list of interesting extensions and open problems.

2 Cross ratios for multipoint correlation functions

As we have explained in the introduction, there is much freedom in introducing sets of independent conformally invariant variables. In this section, we introduce two such sets for multipoint correlation functions. The first one is referred to as polynomial cross ratios

JHEP06(2022)144

and it is a direct generalisation of the common four-point cross ratios u and v to scalar correlators with $N > 4$ field insertions. When written in these cross ratios, all of the $N-3$ quadratic Casimir differential operators that characterise the comb channel multipoint blocks in sufficiently large dimension d turn out to possess polynomial coefficients, at least for $N \leq 10$. The second set of conformal invariants we introduce in this section is fundamental to all of our subsequent discussion. These new coordinates are akin to the variables z and $\bar{z}$ that are widely used for four-point functions. They possess a large number of remarkable properties. Most importantly for us, they behave well under dimensional reductions and when taking OPE limits, which is why we shall also refer to them as *OPE cross ratios*. In addition, these variables possess a nice geometric interpretation.

In the first subsection, the case of $N = 4$ will be briefly reviewed to highlight some of the properties of the cross ratios u, v and $z, \bar{z}$ that make them so useful and are desirable to maintain as we go to a higher number N of insertions. The polynomial cross ratios are then introduced in the second subsection. Next, in the third subsection, we discuss the OPE coordinates for $N = 5$, where there is a single qualitatively new invariant that was already introduced in [34]. The fourth subsection contains the construction of yet another new invariant that is now attached to the central link of the six-point comb channel diagram. We introduce this invariant and provide a geometrical interpretation. The latter is then used to extend the construction of comb channel invariants in $d = 4$ to $N > 6$ insertion points.

2.1 Prologue: cross ratios for four-point blocks

In order to enter the discussion of cross ratios for correlation functions of scalar fields, we will begin with the well known case of $N = 4$ operators. Famously, there exist two independent cross ratios one can build from their four insertions points $x_i, i = 1, \ldots, 4$,

$$u = \frac{x_{12}^2 x_{34}^2}{x_{13}^2 x_{24}^2}\,, \qquad v = \frac{x_{14}^2 x_{23}^2}{x_{13}^2 x_{24}^2}\,. \tag{2.1}$$

These cross ratios can be represented schematically as in Figure 2a, where we disposed the four points along a square and every colored edge corresponds to a scalar product present in the associated cross ratio, with intersecting lines being present in the denominator. When written in these four-point cross ratios u, v, the second order Casimir operator takes the form, see eq. (2.10) in [3],

$$\frac{1}{2}\mathcal{D}_{(12)}^2 = (1-u-v)\partial_v\,(v\partial_v+a+b)+u\partial_u\,(2u\partial_u-d)-(1+u-v)\,(u\partial_u+v\partial_v+a)\,(u\partial_u+v\partial_v+b)\,, \tag{2.2}$$

with the two parameters $2a = \Delta_2 - \Delta_1$ and $2b = \Delta_3 - \Delta_4$ determined by the conformal weights Δ_i of the four external scalar fields. We observe that in these coordinates, the Casimir operator takes a relatively simple form in which all coefficient functions are polynomials in the two cross ratios u and v. But it also has some less pleasant features. In particular, it is not directly amenable to a power series solution in the variables u, v. In order to formalise this a bit more, let us introduce the notion of a *grade* in some variable w. We say that a differential operator of the form $cw^n\partial_w^m$ has w-grade $\mathrm{gr}_w(cw^n\partial_w^m) = n - m$.

JHEP06(2022)144

When the grade is applied to some linear combination of such simple 'monomial' differential operators, it returns a set of grades, one element for each term. For the grades of the Casimir operator (2.2), we find

$$\mathrm{gr}_u\left(\mathcal{D}^2_{(12)}\right) = \{0,1\}\,, \qquad \mathrm{gr}_v\left(\mathcal{D}^2_{(12)}\right) = \{-1,0,1\}\,. \tag{2.3}$$

While the u-grade of the individual terms is non-negative, this is not the case for the v-grade. In other words, when written in the variables u, v, the quadratic Casimir operator contains simultaneously terms that lower and terms that raise the degree of a polynomial in v.

In order to analyse the eigenfunctions of four-point Casimir operators, Dolan and Osborn switched to another parameterisation of the cross ratios through the complex variables z and $\bar{z}$,

$$u = z\bar{z}\,, \qquad v = (1-z)(1-\bar{z})\,. \tag{2.4}$$

We point out that the change of variables is not one-to-one since u and v are invariant under the action of the $\mathbb{Z}_2$ whose non-trivial element exchanges z with $\bar{z}$. Hence, functions of the cross ratios u and v correspond to $\mathbb{Z}_2$ invariant functions of $z, \bar{z}$. The invariants $z, \bar{z}$ possess a nice geometric interpretation. As is well known, conformal transformations can be used to move the insertion points to the special positions $x_2 = 0$, $x_4 = \vec{e}_1$, $x_3 = \infty\vec{e}_1$, where $\vec{e}_1$ denotes the unit vector along the first coordinate direction of the d-dimensional Euclidean space. This choice of a conformal frame is stabilised by a subgroup $\mathrm{SO}(d-1) \subset \mathrm{SO}(d)$ of the rotation group that describes rotations around the first coordinate axis. These rotations can be used to move x_1 into the plane spanned by $\vec{e}_1$ and $\vec{e}_2$. The invariants $z, \bar{z}$ are the complex coordinates of x_1 in this plane. Let us note that in these coordinates, it is very easy to implement the restriction to $d = 1$ for which there exists only one cross ratio, namely $z = \bar{z}$.

The geometric interpretation of the $z, \bar{z}$ coordinates, and in particular their simple reduction to $d = 1$, also manifests itself in another property. Indeed, the so-called Gram determinant of the N insertion points takes a particularly simple form when written in terms of $z, \bar{z}$. Before stating the concrete formula, we need to briefly review the concepts of embedding space and Gram determinants. The embedding space formalism associates a light-like vector $X \in \mathbb{R}^{1,d+1}$ of the form

$$X = \left(\frac{1+x^2}{2}, \frac{1-x^2}{2}, x\right) \in \mathbb{R}^{1,d+1}$$

to any point $x \in \mathbb{R}^d$. The associated light rays are in one-to-one correspondence with points in $\mathbb{R}$. Note that we have chosen a particular representative X of the light ray by fixing the sum of the first two components to $X_{-1} + X_0 = 1$. Given N insertion points x_i, we construct N light-like vectors $X_i \in \mathbb{R}^{1,d+1}$. These vectors are linearly dependent if and only if the associated Gram matrix, that is to say the matrix of scalar products $X_{ij} = \langle X_i, X_j \rangle$, has vanishing determinant. For $N = 4$ points $x_i \in \mathbb{R}^d$, the associated Gram determinant takes the form

$$\det(X_{ij})\big|_4 = (z-\bar{z})^2 X_{13}^2 X_{24}^2\,. \tag{2.5}$$

JHEP06(2022)144

We see that this expression is rather simple when written in terms of the cross ratios $z, \bar{z}$, much simpler than its expression in terms of u, v. Since any four vectors $X_i \in \mathbb{R}^{1,2}$ are linearly dependent, the four-point Gram determinant must vanish in $d = 1$. This is achieved by setting $z = \bar{z}$ so that all four points lie on a single line, in agreement with our discussion in the previous paragraph. The simplicity of the Gram determinant in the $z, \bar{z}$ coordinates means that these are very well suited to implement the dimensional reduction.

Next we turn to a discussion of the Casimir operator. When the expression we spelled out in eq. (2.2) is rewritten in terms of z and $\bar{z}$ it acquires the form, see eq. (2.19) in [3],

$$\begin{aligned}\frac{1}{2}\mathcal{D}^2_{(12)} = z^2(1-z)\frac{\partial^2}{\partial z^2} + \bar{z}^2(1-\bar{z})\frac{\partial^2}{\partial \bar{z}^2} - (a+b+1)\left(z^2\frac{\partial}{\partial z} + \bar{z}^2\frac{\partial}{\partial \bar{z}}\right) \\ - 2ab(z+\bar{z}) + \varepsilon\frac{z\bar{z}}{z-\bar{z}}\left((1-z)\frac{\partial}{\partial z} - (1-\bar{z})\frac{\partial}{\partial \bar{z}}\right),\end{aligned} \tag{2.6}$$

with $\varepsilon = d - 2$. We note that the resulting expression is only slightly longer than for the original set u, v of four-point cross ratios. On the other hand, its coefficients are no longer polynomial. The main advantage of the $z, \bar{z}$ coordinates is that they admit a rather simple implementation of the OPE limit in which we send $\bar{z} \to 0$ first, followed by the limit $z \to 0$. When $|\bar{z}| < |z|$, we can actually expand the last term in the expression for $\mathcal{D}^2_{(12)}$ in a power series. In the resulting expression, all terms possess non-negative $\bar{z}$ grade, i.e.

$$\mathrm{gr}_{\bar{z}}\left(\mathcal{D}^2_{(12)}\right) \in \{0, 1, 2, \dots\}\,. \tag{2.7}$$

This means that there is no term in which the derivatives with respect to $\partial_{\bar{z}}$ outnumber the multiplications with $\bar{z}$. Keeping only terms of vanishing $\bar{z}$-grade, we have

$$\mathcal{D}^2_{(12)} \sim 2z^2(1-z)\frac{\partial^2}{\partial z^2} + 2\bar{z}^2\frac{\partial^2}{\partial \bar{z}^2} - 2(a+b+1)z^2\frac{\partial}{\partial z} - 2abz - 2\varepsilon\bar{z}\frac{\partial}{\partial \bar{z}} + \dots \tag{2.8}$$

In turn, one observes that the terms above all have non-negative z-grade, among which the terms of vanishing grade are given by

$$\mathcal{D}^2_{(12)} \sim 2z^2\frac{\partial^2}{\partial z^2} + 2\bar{z}^2\frac{\partial^2}{\partial \bar{z}^2} - 2\varepsilon\bar{z}\frac{\partial}{\partial \bar{z}} + \dots, \tag{2.9}$$

where now the $\dots$ contain terms of both positive $\bar{z}$- and positive z-grade. Let us now apply this discussion to the problem of finding eigenfunctions of the Casimir operator,

$$\mathcal{D}^2_{(12)}\psi_{\Delta,l}(z,\bar{z}) = \left[\Delta(\Delta-d) + l(l+d-2)\right]\psi_{\Delta,l}(z,\bar{z})\,. \tag{2.10}$$

For the limiting regime in which we replace the Casimir operator by the expression in eq. (2.9), the eigenvalue problem is very easy to solve:

$$\psi_{\Delta,l}(z,\bar{z}) \sim z^{\frac{\Delta+l}{2}}\bar{z}^{\frac{\Delta-l}{2}}c_{\Delta,l} + \dots, \tag{2.11}$$

where $c_{\Delta,l}$ is a non-vanishing constant factor that is not determined by the eigenvalue equation and depends on the normalisation. Since all of the terms omitted from our original

JHEP06(2022)144

Casimir operator have positive grade, we conclude that it possesses an eigenfunction of the form

$$\psi_{\Delta,l}(z,\bar{z}) = z^{\frac{\Delta+l}{2}}\bar{z}^{\frac{\Delta-l}{2}}F_{\Delta,l}(z,\bar{z}) = z^{\frac{\Delta+l}{2}}\bar{z}^{\frac{\Delta-l}{2}}\left(c_{\Delta,l}+O(z,\bar{z})\right), \tag{2.12}$$

i.e. the function F possesses a power series expansion in z and $\bar{z}$ with non-vanishing constant term $c_{\Delta,l}$.

Before we turn to a higher number $N > 4$ of insertion points, we want to summarise a few of the desirable properties of the coordinates $z, \bar{z}$ that are relevant to the rest of the paper. To begin with, when working with multipoint correlators, it is certainly very desirable to have simple expressions for the Gram determinant. Note that N points $X_i \in \mathbb{R}^{1,d+1}$ are linearly dependent whenever $N > d+2$. So if we keep the dimension d fixed, going to larger values of N will inevitably lead to vanishing Gram determinants. Consequently, an N-point function in dimension $d < N-2$ lives on a subspace within the larger space of cross ratios for $d \geq N-2$. The explicit description of this subspace is easiest when working with coordinates in which the Gram determinant factorises into simple functions of the cross ratios. More importantly, we would like to find coordinates that are well adapted to the OPE limit in the sense we outlined above. For higher point functions, this means finding coordinates, subsets of which are associated with the internal links of the OPE diagram, such that eigenfunctions admit a power series expansion in all of the link variables. For $N > 4$, the leading term of these expansions will no longer be constant, of course, but should rather factorise into a product of functions that are associated with the two subdiagrams connected by the link. We will indeed be able to construct such variables for all N-point comb channel diagrams, at least in $d = 4$ dimensions.

2.2 Polynomial cross ratios for comb channel multipoint blocks

In this subsection we address the construction of sets of cross ratios which make all coefficients of comb channel differential operators polynomial. Because of this property, we dub this set *polynomial cross ratios*. We have seen this feature before when writing the Casimir operator for four-point functions in the coordinates u, v, see eq. (2.2). In this sense, the polynomial cross ratios we are about to construct are natural extensions of the four-point cross ratios u, v.

We start be constructing the four-point cross ratios of the same type for each internal link of the comb channel OPE diagram. Consider the link with label $r = 1, \ldots, N-3$. Then the four nearest neighbor insertion points are x_i with $i = r, r+1, r+2, r+3$, see figure 2b. From these we can build two four-point cross ratios u_r, v_r using the same expressions as in the case of four-point functions, i.e. for an N-point comb channel diagram we can construct $(N-3)$ sets of u, v type cross ratios through

$$u_r = \frac{X_{r(r+1)}X_{(r+2)(r+3)}}{X_{r(r+2)}X_{(r+1)(r+3)}}, \qquad v_r = \frac{X_{r(r+3)}X_{(r+1)(r+2)}}{X_{r(r+2)}X_{(r+1)(r+3)}}, \qquad r = 1, \ldots, N-3. \tag{2.13}$$

Here we have used the construction in terms of the embedding space variables X_i, see previous subsection. The $2(N-3)$ cross ratios we have introduced so far do not suffice to generate all conformal invariants as soon as $d > 2$ and $N > 4$. We conjecture that a

JHEP06(2022)144

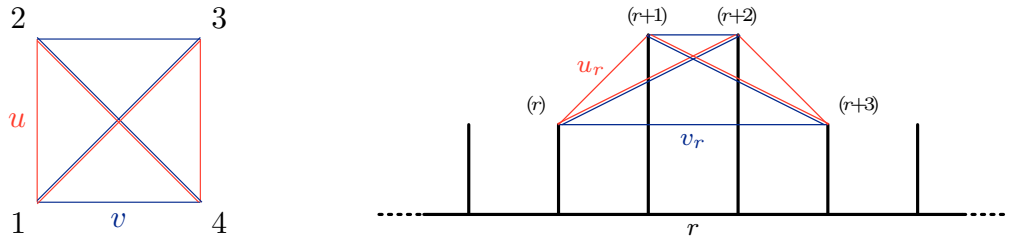

(a) Four-point cross ratios. (b) Construction of four-point cross ratios around internal leg r.

Figure 2: Schematic representation of the four-point cross ratios u and v, where intersecting lines correspond to terms in the denominator. The same type of cross ratios can be constructed around every internal leg by focusing on the closest four points.

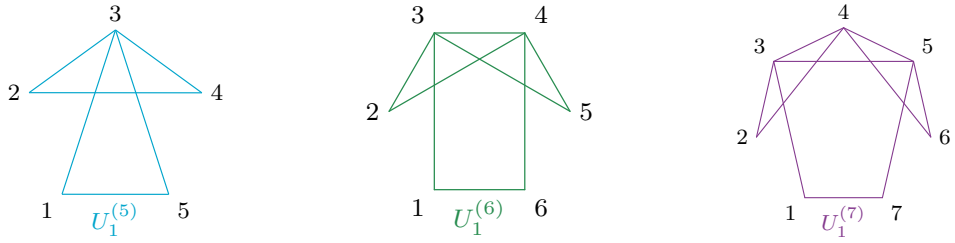

(a) Five-point cross ratio. (b) Six-point cross ratio. (c) Seven-point cross ratio.

Figure 3: Polynomial cross ratios for five, six, and seven point functions. The colored lines correspond to scalar products present in the expression of the cross ratio, with lines that intersect outside vertices corresponding to terms in the denominator.

set of cross ratios making all coefficients of the N-point comb channel Casimir operators polynomial in $d \geq N-2$ is obtained if we complement the four-point cross ratios (u_r, v_r) introduced above by the following set of m-point cross ratios

$$U_s^{(m)} = \frac{X_{s(s+m-1)} \prod_{j=1}^{m-3} X_{(s+j)(s+j+1)}}{\prod_{j=0}^{m-3} X_{(s+j)(s+j+2)}}, \qquad s = 1, \ldots, (N-m+1), \qquad m = 5, \ldots, N. \tag{2.14}$$

The total number of cross ratios we have introduced is $N(N-3)/2$, which coincides with the number of independent cross ratios as long as $d \geq N-2$. We checked our claim of polynomial dependence explicitly by verifying that all comb channel quadratic Casimir operators that appear for up to $N = 10$ external scalar fields indeed have polynomial coefficients in these cross ratios. In addition, we also verified the claim for vertex differential operators with $N \leq 6$. We shall often refer to the variables (2.14) as the *m-point polynomial cross ratios*, since they are constructed around every set of m adjacent points in an N-point function. The first few examples of these type of cross ratios with low values of m are represented schematically in figure 3.

If the dimension d drops below its lower bound or alternatively, if for fixed dimension d the number N of insertion points satisfies $N > d+2$, then there are additional relations between the cross ratios that we have introduced. These can be found by computing the

JHEP06(2022)144

Gram determinant for the scalar products X_{ij}. Given d, the relations allow us to express our m-point cross ratios $U^{(m)}$ with $m > d+2$ in terms of cross ratios involving a lower number of insertion points. In other words, in dimension d, the space of N-point conformal invariants is generated by the cross ratios $U_s^{(m)}$ with $m \leq d+2$. It is easy to verify that the number of such cross ratios indeed coincides with the expected number n_{cr}, see eq. (1.1).

In d dimensions, there are $N-d-1$ of these m-point cross ratios with maximal value $m = d+2$. In particular, the first time one of the latter cross ratios is needed is for $(d+2)$-point functions. For example, to construct the conformal invariants of an N-point function in $d = 3$, we need m-point cross ratios with $m = 4, 5$ only, and the five-point cross ratios first appear for $N = 5$. Similarly, in $d = 4$ dimensions, we work with m-point cross ratios for $m = 4, 5, 6$, and all these invariants appear together starting with $N = 6$ insertion points. Since we are mostly interested in $d = 3, 4$, it will be sufficient for us to analyse Casimir operators for correlation functions of $N = 5$ and $N = 6$ scalar fields.

The set of polynomial cross ratios we have introduced in this subsection leads to relatively simple expressions of Casimir operators, but it does not behave nicely when taking OPE limits of fields, i.e. the OPE limit cannot simply be obtained by taking a limit for a subset of cross ratios to specific values. We will now turn to the construction of new variables that are more suitable for OPE limits.

2.3 Five-point OPE cross ratios

We begin our discussion of the new OPE cross ratios with $N = 5$. As we reviewed above, five insertion points give rise to five independent cross whenever $d \geq 3$. Our recipe for the construction of polynomial cross ratios in the previous subsection provides us with the following set,

$$u_1 = \frac{X_{12}X_{34}}{X_{13}X_{24}}\,, \qquad v_1 = \frac{X_{14}X_{23}}{X_{13}X_{24}}\,, \qquad U_1^{(5)} = \frac{X_{15}X_{23}X_{34}}{X_{24}X_{13}X_{35}}\,. \tag{2.15}$$
$$u_2 = \frac{X_{23}X_{45}}{X_{24}X_{35}}\,, \qquad v_2 = \frac{X_{25}X_{34}}{X_{24}X_{35}}\,,$$

For this case, we already introduced a new parameterisation in [29] through the following set of relations,

$$\begin{aligned} u_1 &= z_1\bar{z}_1\,, & v_1 &= (1-z_1)(1-\bar{z}_1)\,, \\ u_2 &= z_2\bar{z}_2\,, & v_2 &= (1-z_2)(1-\bar{z}_2)\,, \\ U_1^{(5)} &= w_1(z_1-\bar{z}_1)(z_2-\bar{z}_2) + (1-z_1-z_2)(1-\bar{z}_1-\bar{z}_2)\,. \end{aligned} \tag{2.16}$$

Note that the $\mathbb{Z}_2$ symmetry one introduces when passing from u, v to $z, \bar{z}$ for four points is now enhanced to $\mathbb{Z}_2 \times \mathbb{Z}_2$. In the case of five-point functions, the two non-trivial generators of this symmetry act by $z_r \leftrightarrow \bar{z}_r, w_1 \to (1-w_1)$ for $r = 1, 2$. When written in the conformal invariant coordinates $z_r, \bar{z}_r$ and $w = w_1$, the complexity of the differential operators remains roughly on the same level as for the polynomial cross ratios, in the same way as the quadratic Casimir operators for $N = 4$ which have similar complexity in the two sets of

JHEP06(2022)144

variables, cf. eqs. (2.2) and (2.6). But our OPE coordinates for five-point functions have a number of additional properties that are worth pointing out.

To begin with, they possess a rather nice geometric interpretation in a certain conformal frame.[3] Using conformal transformations, it is possible to move three points, let's say x_2, x_3 and x_4, onto a single line with positions $0, 1, \infty$. Then we can use the remaining rotations transverse to that line in order to move x_1 into a plane, and finally rotations transverse to that plane in order to move x_5 into some 3-dimensional subspace. Thus, there exists a conformal transformation $g^{(5)}$ such that

$$\begin{aligned} g^{(5)}(x_1) &= \varrho_1 \left(\cos\theta_1, \sin\theta_1, 0, \vec{0}\right) , & g^{(5)}(x_2) &= \left(0, 0, 0, \vec{0}\right) , \\ g^{(5)}(x_3) &= \left(\infty, 0, 0, \vec{0}\right) , & g^{(5)}(x_4) &= \vec{e}_1 = \left(1, 0, 0, \vec{0}\right) , \\ g^{(5)}(x_5) &= e_1 - \varrho_2 \left(\cos\theta_2, \sin\theta_2 \cos\phi, \sin\theta_2 \sin\phi, \vec{0}\right) . \end{aligned} \tag{2.17}$$

Here we have parameterised the image point $g^{(5)}(x_1)$ in the plane through an angle θ_1 and a distance ϱ_1, as usual. Similarly, we have also parameterised the point $g^{(5)}(x_5)$ in a 3-dimensional space through two angles θ_2, ϕ and one distance ϱ_2, using $g^{(5)}(x_4) = \vec{e}_1$ as reference point. In all of these expressions, $\vec{0}$ denotes a vector with $d-3$ vanishing components. We note that in $d = 4$ dimensions, the conformal transformation $g^{(5)}$ is uniquely fixed by our choice of frame. It is now easy to compute our new variables $z_r, \bar{z}_r$ and w_1 in terms of θ_r, ϱ_r and ϕ,

$$z_1 = \varrho_1 e^{\mathrm{i}\theta_1} , \qquad \bar{z}_1 = \varrho_1 e^{-\mathrm{i}\theta_1} , \qquad z_2 = \varrho_2 e^{\mathrm{i}\theta_2} , \qquad \bar{z}_2 = \varrho_2 e^{-\mathrm{i}\theta_2} , \qquad w_1 = \sin^2\frac{\phi}{2} . \tag{2.18}$$

This is illustrated in figure 4. In particular we see that z_1, $\bar{z}_1$ and z_2, $\bar{z}_2$ describe the two planes $x_1x_2x_3x_4$ and $x_2x_3x_4x_5$ respectively, while w_1 is a function of the angle ϕ between those planes. As can be read off from this picture, the domain of w_1 in Euclidean signature is

$$w_1 \in [0, 1] . \tag{2.19}$$

The description we provided is valid for $d \geq 3$. As we go down to $d = 2$, there are no longer enough dimensions in order to have a non-vanishing angle ϕ between two 2-planes, i.e. we must set $\phi = 0$ or $\phi = \pi$ and hence $w_1 = 0$ or $w_1 = 1$. As in our review of four-point functions, we expect to recover these values of w_1 as zeroes of the Gram determinant. And indeed, the Gram determinant for the five coordinates X_i acquires the following form,

$$\det(X_{ij})\big|_5 = 2\frac{w_1\,(1-w_1)\,(z_1-\bar{z}_1)^2\,(z_2-\bar{z}_2)^2\,X_{13}^2 X_{24}^2 X_{35}^2}{X_{23}X_{34}} . \tag{2.20}$$

In addition to the two factors w_1 and $w_1 - 1$, we also notice the zeros that appear for $z_r = \bar{z}_r$, i.e. when the four points $x_1x_2x_3x_4$ or $x_2x_3x_4x_5$ lie on a line.

In section 4.2 of [34], we also used these coordinates to analyse the OPE limit of our Gaudin differential operators. This analysis showed clearly how the variable w_1 is

[3] We thank Luke Corcoran for pointing out this frame to us.

JHEP06(2022)144

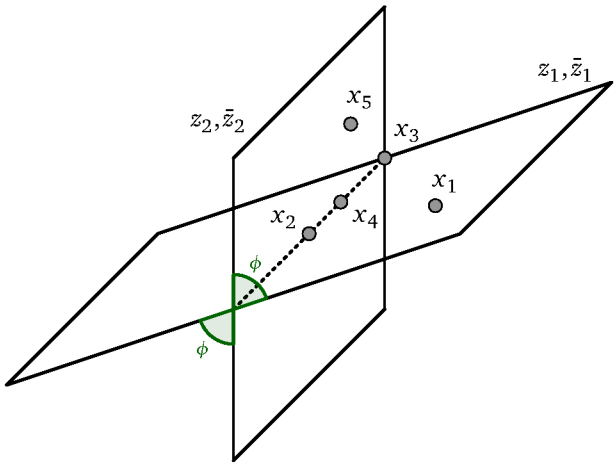

Figure 4: Conformal frame for five points.

naturally associated with the degree of freedom describing the choice of tensor structures at the internal vertex of a five-point OPE diagram. More specifically, we took the OPE limit for the two sets $z_1, \bar{z}_1$ and $z_2, \bar{z}_2$ of variables associated with the two internal links of the OPE diagram. In the limit where we take $\bar{z}_r \to 0$ first, followed by $z_r \to 0$, the joint eigenfunctions of the five differential operators behave as

$$\psi_{\Delta_r, l_r; \kappa}(z_r, \bar{z}_r, w_1) \sim \prod_{r=1}^{2} z_r^{\frac{\Delta_r + l_r}{2}} \bar{z}_r^{\frac{\Delta_r - l_r}{2}} \left(\gamma_{\Delta_r, l_r; \kappa}(w_1) + O(z_r, \bar{z}_r)\right) . \tag{2.21}$$

The derivation follows the same steps outlined in the discussion of four-point blocks in the first subsection. But in contrast to the case of $N = 4$, the leading term γ of the power series expansion in $z_r, \bar{z}_r$ is no longer constant, but rather an eigenfunction of a single variable vertex differential operator for an STT-STT-scalar three-point function, which we constructed and analysed in [34]. The latter was shown to arise in the OPE limit of the five-point vertex operator, which acts on all the five cross ratios before taking the limit. The STT-STT-scalar three-point function is determined by conformal symmetry up to a function of a single variable. The latter can be constructed in terms of the standard $2, 3$-point tensor structures H_{ij} and $V_{i,jk}$ of [38]. The detailed comparison of the 3-point with the OPE limit of the five-point vertex operators gives

$$w_1 \to 1 - \frac{H_{ab}}{V_{a,3b} V_{b,a3}} , \tag{2.22}$$

where a and b are the internal legs on which the OPE limit projects, see [34] for a detailed discussion.

JHEP06(2022)144

2.4 Six-point OPE cross ratios

Having reviewed our parameterisation of five-point cross ratios, we now turn to a discussion of $N = 6$. As long as $d \geq 4$, our set of independent polynomial cross ratios consists of

$$u_3 = \frac{X_{34}X_{56}}{X_{35}X_{46}}\,, \qquad v_3 = \frac{X_{45}X_{36}}{X_{35}X_{46}}\,, \qquad U_2^{(5)} = \frac{X_{26}X_{34}X_{45}}{X_{35}X_{24}X_{46}}\,, \tag{2.23}$$

$$U_1^{(6)} = \frac{X_{16}X_{23}X_{34}X_{45}}{X_{13}X_{24}X_{35}X_{46}}\,, \tag{2.24}$$

in addition to the five cross ratios already introduced in eq. (2.15). While the three cross ratios in the first line are of the same type as those we met in our discussion of $N = 5$, the six-point cross ratio in the second line is fundamentally new. In passing to our OPE coordinates, it is natural to make use of the map (2.16) for those cross ratios shared with the previously discussed five-point function, while analogously mapping the cross ratios in eq. (2.23) to

$$\begin{aligned} u_3 &= z_3\bar{z}_3\,, \qquad v_3 = (1-z_3)(1-\bar{z}_3)\,, \\ U_2^{(5)} &= w_2(z_2-\bar{z}_2)(z_3-\bar{z}_3) + (1-z_2-z_3)(1-\bar{z}_2-\bar{z}_3)\,. \end{aligned} \tag{2.25}$$

For the six-point variable (2.24), a new type of mapping is necessary. In the same way that the variables z_r, $\bar{z}_r$ are associated with exchanges of STTs, and the w_s variables are associated with specific non-trivial tensor structures sitting at internal vertices of OPE diagrams, the new variable we want to introduce should be associated with exchanges of Mixed-Symmetry Tensors with two spins, and it should naturally combine with the z_2, $\bar{z}_2$ cross ratios to make up the three exchanged degrees of freedom of the middle link. We propose to introduce this conformal invariant $\Upsilon = \Upsilon_2$ via the relation

$$\begin{aligned} U_1^{(6)} = {} & \Upsilon\,(z_1-\bar{z}_1)\,(z_2-\bar{z}_2)\,(z_3-\bar{z}_3)\,\sqrt{w_1(1-w_1)w_2(1-w_2)} - w_1w_2\,(z_1-\bar{z}_1)\,(\bar{z}_2+z_2)\,(z_3-\bar{z}_3) \\ & + w_1\,(z_1-\bar{z}_1)\,[z_2\,(1-\bar{z}_3)-\bar{z}_2(1-z_3)] + w_2\,(z_3-\bar{z}_3)\,[z_2\,(1-\bar{z}_1)-\bar{z}_2(1-z_1)] \\ & + [z_2-(1-z_1)(1-z_3)]\,[\bar{z}_2-(1-\bar{z}_1)(1-\bar{z}_3)]\,. \end{aligned} \tag{2.26}$$

The new variables $z_r, \bar{z}_r, w_s$ and Υ admit an action of $\mathbb{Z}_2^3$ that leaves the original cross ratios invariant. The nontrivial elements σ_r of the three $\mathbb{Z}_2$ factors each exchange one of the pairs $z_r \leftrightarrow \bar{z}_r$, map $w_s \to (1-w_s)$ for $r = s, s+1$ and send Υ to $-\Upsilon$.

As a first quick test of our proposal, we can compute the six-point Gram determinant. When expressed in the OPE coordinates, it reads

$$\det\left(X_{ij}\right)\big|_6 = \frac{(1-w_1)\,w_1\,(1-w_2)\,w_2\,(z_1-\bar{z}_1)^2\,(z_2-\bar{z}_2)^2\,(z_3-\bar{z}_3)^2\,(4z_2\bar{z}_2-\Upsilon^2\,(z_2-\bar{z}_2)^2)}{z_2^2\bar{z}_2^2}\,\frac{\prod_{i=1}^4 X_{i,i+1}^2}{X_{34}^2}\,. \tag{2.27}$$

Given the lengthy relation between the six-point cross ratio $U^{(6)}$ and Υ it is very reassuring to see that the Gram determinant now fits into a single line. In addition, the new conformal invariant Υ appears in a single factor, combined only with the cross ratios $z_2, \bar{z}_2$. If we

JHEP06(2022)144

reduce the dimension to $d = 3$, the number of cross ratios drops by one. In our new set of conformal invariants, we see that Υ can then be expressed in terms of $z_2, \bar{z}_2$ as

$$\Upsilon^2 = \frac{4 z_2 \bar{z}_2}{(z_2 - \bar{z}_2)^2} \quad \textit{for} \quad d = 3. \tag{2.28}$$

All these simple relations are quite remarkable. On the other hand, they are not yet sufficient to fully appreciate our definition of Υ. For example, given what we have seen, one may still wonder why we did not rescale Υ to make the last bracket in the Gram determinant equal to $(\Upsilon^2 - 1)$. While that is certainly possible, and leads to a nicer geometrical interpretation, the rescaled variable would result in more complicated expressions for the asymptotics of comb channel blocks in OPE limits, see our discussion in the next section.

The interpretation of our coordinates proceeds as in the previous subsection. In that case, each of the two internal links was associated with a complex plane. We used the coordinates $z_1, \bar{z}_1$ and $z_2, \bar{z}_2$ to specify two positions on these two planes and related the variable w_1 to the relative angle between the two planes within a 3-dimensional subspace. As we go to $N = 6$, the same picture applies, but with dimensions raised by one. Instead of the 2-planes in 3-space, we now have two 3-spaces that are associated with the points $x_1, \ldots, x_5$ and $x_2, \ldots, x_6$, respectively. These are embedded in a 4-dimensional subspace with the relative angle being measured by a new angle φ. Each of the two 3-spaces contains the configuration of two planes depicted in figure 4. For the first five points $x_1, \ldots, x_5$, this defines the coordinates $\varrho_1, \theta_1, \varrho_2, \theta_2$ and ϕ as before. We obtain a similar set of coordinates for the second set $x_2, \ldots, x_6$. Now it is easy to see that one pair of coordinates coincides with the ones from the first quintuple of insertion points, so that in total we need eight coordinates $\varrho_r, \theta_r, \phi_1, \phi_2$ with $r = 1, 2, 3$ to parameterise the configurations within each of the 3-spaces. With these coordinates, one finds that

$$z_r := \varrho_r e^{\mathrm{i}\theta_r}, \qquad w_s := \sin^2 \frac{\phi_s}{2}, \qquad \Upsilon := \pm \mathrm{i} \frac{\cos\varphi}{\sin\theta_2}, \tag{2.29}$$

where $r = 1, 2, 3$ and $s = 1, 2$. The sign in Υ is conventional, and can be absorbed in a shift of the angle φ. A more formal definition of the various geometric parameters on the right hand side will be given in the next subsection as part of a more general construction that applies to any number N of points in $d = 4$ dimensions.

2.5 Generalisation to higher number of points

In order to extend our choice of coordinates to higher number N of insertion points in $d = 4$ dimensions, it is useful to formalise the construction we have described at the end of the previous subsection. As described in subsection 2.3, each quintuple of consecutive points $x_s, x_{s+1}, \ldots, x_{s+4}$ defines a conformal transformation $g_s^{(5)}$ as in eq. (2.17),

$$\begin{aligned}
g_s^{(5)}(x_s) &=: \varrho_s \vec{n}(\theta_s, 0)\,, & g_s^{(5)}(x_{s+1}) &=: (0,0,0,0), \\
g_s^{(5)}(x_{s+2}) &=: (\infty,0,0,0)\,, & g_s^{(5)}(x_{s+3}) &=: \vec{e}_1 = (1,0,0,0), \\
g_s^{(5)}(x_{s+4}) &=: \vec{e}_1 - \varrho_{s+1}\vec{n}(\theta_{s+1}, \phi_s), & &
\end{aligned} \tag{2.30}$$

where $s = 1, \ldots, N-4$ and we defined the unit vectors $\vec{n}$ as

$$\vec{n}(\theta, \phi) := (\cos\theta, \sin\theta\cos\phi, \sin\theta\sin\phi, 0). \tag{2.31}$$

Thus, to compute x_6 in the conformal frame where $g_1^{(5)}(x_1), \ldots, g_1^{(5)}(x_5)$ are of the form (2.17), we express the sixth point as

$$g_1^{(5)}(x_6) = g_1^{(5)} \circ g_2^{(5)-1}(\vec{e}_1 - \varrho_3 \vec{n}(\theta_3, \phi_2)) \equiv h_{12}^{(5)}(\vec{e}_1 - \varrho_3 \vec{n}(\theta_3, \phi_2)). \tag{2.32}$$

By construction, $h_{12}^{(5)}$ is a conformal group element parameterised by the cross ratios of the six-point function. In appendix B, we compute this conformal transformation and find

$$h_{12}^{(5)-1} = \varrho_2^{-D} \mathcal{I}\sigma_1 e^{-\varphi M_{34}} e^{-\theta_2 M_{12}} e^{-\phi_1 M_{23}} e^{P_1}, \tag{2.33}$$

where $\mathcal{I}$ is conformal inversion and $\sigma_1 : (x^1, x^2, x^3, x^4) \mapsto (-x^1, x^2, x^3, x^4)$ is a reflection along the hyperplane orthogonal to the first coordinate direction. The explicit action of the element (2.33) on spacetime points x is given by

$$h_{12}^{(5)-1}(x) = \varrho_2 \sigma_1 e^{-\varphi M_{34}} e^{-\theta_2 M_{12}} e^{-\phi_1 M_{23}} \frac{x - \vec{e}_1}{(x - \vec{e}_1)^2}. \tag{2.34}$$

In particular, we read off from there that the angle φ describes the relative angle between two 3-spaces. It is obvious how to continue these constructions beyond $N = 6$ points in $d = 4$. We continue to introduce comb channel cross ratios $z_r, \bar{z}_r$ and w_s in terms of the polynomial cross ratios through relations (2.16) with indices running over $r = 1, \ldots, N-3$ and $s = 1, \ldots N-4$, respectively. Similarly, we introduce Υ_r with $r = 2, \ldots N-4$ through relations of the form (2.26). After extending our relations (2.29) to a higher number of comb channel OPE coordinates we introduce the geometric coordinates as

$$z_r := \varrho_r e^{\mathrm{i}\theta_r}, \quad w_s := \sin^2\frac{\phi_s}{2}, \quad \Upsilon_r := \pm\mathrm{i}\frac{\cos\varphi_r}{\sin\theta_{r+1}}, \tag{2.35}$$

and define in direct analogy to eq. (2.33) the conformal transformations

$$h_{s(s+1)}^{(5)} := g_s^{(5)} \circ g_{s+1}^{(5)-1} = \varrho_{s+1}^{-D} \mathcal{I}\sigma_1 e^{-\varphi_s M_{34}} e^{-\theta_{s+1} M_{12}} e^{-\phi_s M_{23}} e^{-\varphi_{s-1} M_{34}} e^{P_1}, \tag{2.36}$$

for $s = 1, \ldots, N-4$. We can thus supplement eqs. (2.30) by the relations

$$\begin{aligned}
g_1^{(5)}(x_6) &= h_{12}^{(5)}(\vec{e}_1 - \varrho_3 \vec{n}(\theta_3, \phi_2)), \\
g_1^{(5)}(x_7) &= h_{23}^{(5)} \circ h_{12}^{(5)}(\vec{e}_1 - \varrho_4 \vec{n}(\theta_4, \phi_3)) \\
&\cdots \\
g_1^{(5)}(x_N) &= h_{(N-5)(N-4)}^{(5)} \circ h_{(N-6)(N-5)}^{(5)} \circ \cdots \circ h_{23}^{(5)} \circ h_{12}^{(5)}(\vec{e}_1 - \varrho_{N-3} \vec{n}(\theta_{N-3}, \phi_{N-4})).
\end{aligned}$$

These formulas allow us to compute the location of the insertion points in the conformal frame defined by the first five points $x_1, \ldots, x_5$, see eq. (2.30), in terms of the geometric parameters $\varrho_r, \theta_r, \phi_s$ and φ_r. The latter possess a very simple relation with the OPE cross ratios that we spelled out in eq. (2.35).

JHEP06(2022)144

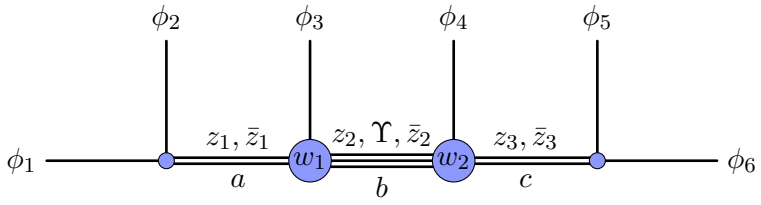

Figure 5: Six point function with external scalars in the comb channel. The z_i, $\bar{z}_i$, w_i and Υ type of cross ratios are naturally associated with one particular internal leg or vertex of the OPE diagram.

3 OPE limits and factorisation for six-point blocks

In the previous section, we introduced new conformally invariant coordinates for multipoint blocks in $d = 4$ dimensions that were naturally attached to the links and vertices of a comb channel OPE diagram, see e.g. figure 5 for the example of $N = 6$. To support our choice, we provided a nice geometric interpretation and, closely related, showed that the Gram determinant for $N = 6$ points admits a simple factorised expression, see eq. (2.27). Recall that the six-point function in $d \leq 4$ is the first correlator for which the new link variable Υ appears. This makes $N = 6$ the decisive case when it comes to testing our cross ratios for comb channel blocks in $d = 4$. The next two sections are devoted to the most important test.

As we have reviewed in subsection 2.1, what makes the cross ratios $z, \bar{z}$ for 4-point function so useful is the fact that they provide power series expansions in the OPE limit where $z, \bar{z}$ go to zero. One can deduce this important feature from the expressions of the Casimir differential operators. Here we want to extend this type of analysis to the OPE limits of six-point functions and in particular, to the limit in which the coordinates $z_2, \bar{z}_2$ and Υ attached to the central link of the comb channel diagram are sent to zero. Our goal is to show that in this limit, the six-point comb channel blocks possess a power series expansion, and that the leading term of this expansion factorises into a product of two functions, one depending on $z_1, \bar{z}_1, w_1$, the other on $z_3, \bar{z}_3, w_2$.

In our approach, we characterise multipoint blocks as eigenfunctions of a complete set of commuting differential operators. For $N = 6$ comb channel blocks, these operators are briefly reviewed in the first subsection. Then we show that the OPE limit we are interested in does indeed correspond to sending $z_2, \bar{z}_2$ and Υ to zero. In the final subsection, we then perform the OPE limit on the differential operators, and show that these operators decouple into two independent sets associated with the left and right side of the diagram. We also provide concrete expressions for the limiting differential operators. These will be further analysed in the next section.

3.1 Preliminaries on comb channel six-point blocks

In this subsection, we shall specify all of our conventions concerning six-point blocks and the differential operators we use to characterise them. As usual, any six-point correlation function of scalar fields can be split into a product of some homogeneous prefactor Ω, which

JHEP06(2022)144

depends on the scaling weights Δ_i and insertion points x_i of the external scalar fields, and a function F of the nine cross ratios,

$$\langle\phi_1\phi_2\phi_3\phi_4\phi_5\phi_6\rangle = \Omega_6^{(\Delta_i)}(X_i)\, F^{(\Delta_i)}\Big(u_1,v_1,u_2,v_2,u_3,v_3,U_1^{(5)},U_2^{(5)},U_1^{(6)}\Big)\,. \tag{3.1}$$

The prefactor is not unique.[4] Here we shall adopt the following choice:

$$\Omega_6^{(\Delta_i)}(X_i) = \frac{1}{X_{12}^{\frac{\Delta_1+\Delta_2}{2}} X_{34}^{\frac{\Delta_3+\Delta_4}{2}} X_{56}^{\frac{\Delta_5+\Delta_6}{2}}} \left(\frac{X_{23}}{X_{13}}\right)^{\frac{\Delta_1-\Delta_2}{2}} \left(\frac{X_{24}}{X_{23}}\right)^{\frac{\Delta_3}{2}} \left(\frac{X_{35}}{X_{45}}\right)^{\frac{\Delta_4}{2}} \left(\frac{X_{45}}{X_{46}}\right)^{\frac{\Delta_6-\Delta_5}{2}}\,. \tag{3.2}$$

The function $F^{(\Delta_i)}$ admits a conformal block decomposition of the form

$$F^{(\Delta_i)} = \sum_{\Xi} \Lambda_\Xi\, \psi_\Xi^{(\Delta_i)}\left(u_r,v_r,U_1^{(5)},U_2^{(5)},U_1^{(6)}\right), \quad \textit{where} \quad \Xi = \{\Delta_a,l_a,\Delta_b,l_b,\ell_b,\Delta_c,l_c,\tau_L,\tau_R\} \tag{3.3}$$

is a complete set of quantum numbers that includes the weights $\Delta_a,\Delta_b,\Delta_c$ and spins l_a,l_b,ℓ_b,l_c of the internal fields in the comb channel decomposition, as well as two quantum numbers τ_L and τ_R that label the choice of tensor structure at the two central vertices of the diagram in figure 5. We have also split each summand into a product of OPE coefficients $\Lambda = \Lambda_\Xi$ and a conformal block ψ_Ξ. From now on, we will drop the labels on ψ, unless they are not clear from the context in which ψ appears.

The six-point comb channel conformal blocks in eq. (3.3) are joint eigenfunctions of nine differential operators, as was shown in [29]. These include three quadratic Casimir operators, which are constructed for each of the three internal links of the OPE diagram as

$$\mathcal{D}^2_{(12)} = (\mathcal{T}_1+\mathcal{T}_2)_{[AB]}(\mathcal{T}_1+\mathcal{T}_2)^{[BA]} = \mathcal{D}^2_{(3456)}\,, \tag{3.4}$$

$$\mathcal{D}^2_{(123)} = (\mathcal{T}_1+\mathcal{T}_2+\mathcal{T}_3)_{[AB]}(\mathcal{T}_1+\mathcal{T}_2+\mathcal{T}_3)^{[BA]} = \mathcal{D}^2_{(456)}\,, \tag{3.5}$$

$$\mathcal{D}^2_{(56)} = (\mathcal{T}_5+\mathcal{T}_6)_{[AB]}(\mathcal{T}_5+\mathcal{T}_6)^{[BA]} = \mathcal{D}^2_{(1234)}\,. \tag{3.6}$$

Here we have adopted the standard convention to label the generators $\mathcal{T}_\alpha$ of the conformal algebra through pairs AB with $A,B = 1,\ldots,d+2$ such that $\mathcal{T}_{AB} = -\mathcal{T}_{BA}$. The three quadratic Casimir operators are joined by three quartic ones that take the following form,

$$\mathcal{D}^4_{(12)} = (\mathcal{T}_1+\mathcal{T}_2)_{[AB]}(\mathcal{T}_1+\mathcal{T}_2)^{[BC]}(\mathcal{T}_1+\mathcal{T}_2)_{[CD]}(\mathcal{T}_1+\mathcal{T}_2)^{[DA]} = \mathcal{D}^4_{(3456)}\,, \tag{3.7}$$

$$\mathcal{D}^4_{(123)} = (\mathcal{T}_1+\mathcal{T}_2+\mathcal{T}_3)_{[AB]}(\mathcal{T}_1+\mathcal{T}_2+\mathcal{T}_3)^{[BC]}(\mathcal{T}_1+\mathcal{T}_2+\mathcal{T}_3)_{[CD]}(\mathcal{T}_1+\mathcal{T}_2+\mathcal{T}_3)^{[DA]} = \mathcal{D}^4_{(456)}\,, \tag{3.8}$$

$$\mathcal{D}^4_{(56)} = (\mathcal{T}_5+\mathcal{T}_6)_{[AB]}(\mathcal{T}_5+\mathcal{T}_6)^{[BC]}(\mathcal{T}_5+\mathcal{T}_6)_{[CD]}(\mathcal{T}_5+\mathcal{T}_6)^{[DA]} = \mathcal{D}^4_{(1234)}\,. \tag{3.9}$$

In addition, there is one third-order Pfaffian operator that is assigned to the central link,

$$\mathcal{D}^3_{(123)} = \epsilon^{ABCDEF}(\mathcal{T}_1+\mathcal{T}_2+\mathcal{T}_3)_{[AB]}(\mathcal{T}_1+\mathcal{T}_2+\mathcal{T}_3)_{[CD]}(\mathcal{T}_1+\mathcal{T}_2+\mathcal{T}_3)_{[EF]}\,. \tag{3.10}$$

[4] This liberty is $\Omega \mapsto \Omega\Theta^{-1}$, $\psi \mapsto \Theta\psi$, where Θ is a non-singular function of the cross ratios. However, after imposing the specific power law asymptotics (1.6) for the blocks in the OPE limit at each internal leg, our prefactor is a natural choice.

JHEP06(2022)144

To complete the list of differential operators, we finally spell out the two fourth order vertex operators,

$$\mathcal{D}^{4,3}_{L,(12)3} = (\mathcal{T}_1 + \mathcal{T}_2)_{[AB]}(\mathcal{T}_1 + \mathcal{T}_2)^{[BC]}(\mathcal{T}_1 + \mathcal{T}_2)_{[CD]}(\mathcal{T}_3)^{[DA]}\,, \tag{3.11}$$

$$\mathcal{D}^{4,3}_{R,(56)4} = (\mathcal{T}_5 + \mathcal{T}_6)_{[AB]}(\mathcal{T}_5 + \mathcal{T}_6)^{[BC]}(\mathcal{T}_5 + \mathcal{T}_6)_{[CD]}(\mathcal{T}_4)^{[DA]}\,. \tag{3.12}$$

In the following, we will mostly focus on the quadratic Casimir operators. It is rather easy to compute the expression of these Casimir operators in the polynomial cross ratios with the aid of computer algebra software and verify that of all their coefficients are indeed polynomial, as we had claimed in the previous section. The resulting expressions for Casimir operators are actually the simplest we have been able to find, simpler than for any other set of coordinates. On the other hand, the polynomial cross ratios are not well adapted to taking OPE limits, as we will argue in section 3.3. Taking the OPE limit will require passing to the new OPE coordinates introduced in the previous section.

3.2 The OPE limit from embedding space

Our goal now is to motivate why we expect the sum over descendants in the central intermediate link to be encoded in a power series expansion in the variables $z_2, \bar{z}_2, \Upsilon$. The idea here is to prepare the intermediate fields through an operator product expansion of either the three fields on the left, or the three fields on the right of the central link. For the left hand side, this amounts to making x_1, x_2 and x_3 collide.

It is a little more tricky to understand how the OPE limit is performed once we pass to the cross ratios. As an example, let us briefly look at the limit in which x_1 and x_2 come together. In the process, we expect to go from a six-point function of scalar fields to a five-point function with one STT insertion and four scalars. While the former has nine cross ratios, the latter has only seven, i.e. we expect that two cross ratios are fixed in the OPE limit. On the other hand, if we apply the limit to the nine polynomial cross ratios we find

$$u_1 \to 0\,, \qquad v_1 \to 1\,, \qquad U_1^{(5)} \to v_2\,, \qquad U_1^{(6)} \to U_2^{(5)}\,. \tag{3.13}$$

Of course, this simply means that one needs to consider subleading terms in the limiting behaviour of the cross ratios in order to parameterise the seven cross ratios of the resulting five-point function. But it does illustrate how subtle OPE limits are in the space of cross ratios.

In order to analyse the triple OPE limits of our new cross ratios, it is advantageous to work in embedding space. In the next few paragraphs, we will review how to take double limits into STTs and triple limits into MSTs. When dealing with computations in embedding space, we will work in a Poincaré patch in which the sum $X_{-1} + X_0$ of the first two entries is nonzero. We can then associate the following lightlike vector $X \in \mathbb{R}^{1,d+1}$ with the usual Minkowski metric to any insertion point $x \in \mathbb{R}^d$,

$$X = \left(\frac{1+x^2}{2}, \frac{1-x^2}{2}, x\right), \tag{3.14}$$

JHEP06(2022)144

where we use rescalings to set $X_{-1} + X_0 = 1$. This amounts to working with a particular representative of the projective lightray defined by x. To describe STTs, we additionally need polarisation vectors Z that take the form

$$Z = (x \cdot z, -x \cdot z, z)\,, \qquad z = \left(\frac{1-\zeta^2}{2}, \mathrm{i}\frac{1+\zeta^2}{2}, \zeta\right) \in \mathbb{C}^d \tag{3.15}$$

Here $\zeta \in \mathbb{C}^{d-2}$ describes the physical degrees of freedom of the polarisation. These are first mapped to a vector $z \in \mathbb{C}^d$ that satisfies $z^2 = 0$. We think of z as describing a direction in $\mathbb{C}^d$ and use rescalings to set $z_1 + \mathrm{i}z_2 \equiv 1$. In the last step, we complement z into a vector Z with $d+2$ components. As one can easily verify, the vector Z satisfies light cone and transversality conditions of the form $Z^2 = 0 = X \cdot Z$.

When dealing with MST fields, finally, we need a second polarisation W. It has $d-4$ physical degrees of freedom, which we describe through a null vector $\omega \in \mathbb{C}^{d-2}$, $\omega^2 = 0$, normalised to $\omega_1 + \mathrm{i}\omega_2 \equiv 1$,

$$W = (x \cdot w, -x \cdot w, w)\,, \qquad w = (\zeta \cdot \omega, -i\zeta \cdot \omega, \omega) \in \mathbb{C}^d\,. \tag{3.16}$$

By construction, W is lightlike and transversal to both X and Z, i.e. $W^2 = 0 = X \cdot W = Z \cdot W$. With this notation in place, we spell out below the procedure to follow when taking OPE limits in embedding space, for each of the relevant cases.

To discuss the OPE limit of a pair of scalars inserted at x_1 and x_2, we use their embedding space coordinates X_1 and X_2. Projecting to the STTs that are produced by the OPE of those two scalar fields requires us to construct the embedding space coordinate X_{STT} and polarisation Z_{STT} of said fields from the coordinates of the two scalars. This can be achieved by first taking a lightcone limit $X_1 \cdot X_2 = 0$. Once the lightcone condition is satisfied, we introduce

$$X_{\mathrm{STT}} = \frac{1}{2}(X_1 + X_2)\,, \qquad Z_{\mathrm{STT}} = \frac{1}{(X_2 - X_1)_1 + \mathrm{i}(X_2 - X_1)_2}(X_2 - X_1)\,. \tag{3.17}$$

Note that the prefactor in the definition of Z_{STT} ensures that the polarisation is normalised such that $z_1 + \mathrm{i}z_2 = 1$. Thanks to the condition $X_1 \cdot X_2 = 0$, the two vectors we have built from X_1 and X_2 satisfy the usual relations for STT variables, namely $X_{\mathrm{STT}}^2 = 0 = Z_{\mathrm{STT}}^2$ and $X_{\mathrm{STT}} \cdot Z_{\mathrm{STT}} = 0$. So far, we have only assumed that the two insertion points of scalar fields are light-like separated, so that $X_1 \cdot X_2 = 0$. To complete the OPE limit, we can now set $X_2 = X_1 + \epsilon\, Z_{\mathrm{STT}}$ and compute the $\epsilon \to 0$ limit.

In order to address the triple OPE limit, it remains to discuss the operator product of an STT with a scalar field. Let us consider an STT with associated coordinates X_1, Z_1 and a scalar at position X_2. If we want to project to the exchange of an MST_2 produced by their OPE, we need to construct embedding space coordinates X_{MST_2} and polarisations $Z_{\mathrm{MST}_2}, W_{\mathrm{MST}_2}$ starting from the degrees of freedom of the two initial fields. To this end, we will follow a nested procedure with two limits of the type described above. As before, we start by taking the lightcone limit $X_1 \cdot X_2 = 0$ and construct the expressions

$$X_{\mathrm{MST}_2} = \frac{1}{2}(X_1 + X_2)\,, \qquad Z' = \frac{1}{(X_2 - X_1)_1 + \mathrm{i}(X_2 - X_1)_2}(X_2 - X_1)\,. \tag{3.18}$$

JHEP06(2022)144

From here, one can take $X_2 = X_1 + \epsilon\, Z'$ and compute the $\epsilon \to 0$ limit. This leads temporarily to something described by one coordinate X_{MST_2} and two auxiliary vectors of STT type Z_1 and Z'. Finally, to make this set suitable to describe an MST_2, we take the lightcone limit $Z' \cdot Z_1 = X_2 \cdot Z_1 = 0$ and construct

$$Z_{\mathrm{MST}_2} = \frac{1}{2}\,(Z' + Z_1)\,, \qquad W_{\mathrm{MST}_2} = \frac{1}{(Z'-Z_1)_3 + \mathrm{i}\,(Z'-Z_1)_4}\,(Z' - Z_1)\,. \tag{3.19}$$

These two vectors indeed satisfy the appropriate conditions for polarisations associated with an MST_2 and the normalisation matches that of the introduction. At this point, we can complete the OPE limit by writing $Z' = Z + \epsilon W$ and taking $\epsilon \to 0$.

Let us now come back to the cross ratios and analyse their behaviour when in the OPE limit. This is particularly simple for the OPE of two scalar fields ϕ_1 and ϕ_2, in which case one finds that $\bar{z}_1$ and z_1 both tend to zero while all other cross ratios remain finite. A similar statement holds for the OPE limit of the two scalar field ϕ_5 and ϕ_6. It is less straightforward to understand the leading behaviour for exchanges of an MST_2 at the internal leg in the middle. To study this, let us start by taking the OPE limit on the left side of the OPE diagram and reducing to a five-point function of fields $\mathcal{O}_a$, $\phi_3, \ldots, \phi_6$. Here, the OPE limit for leg b can simply be cast as a limit for one STT with coordinates X_a, Z_a and one scalar with coordinate X_3, of the form described in section 3.2. Following that procedure, it is possible to check that

$$w_1 \xrightarrow{((12)3)\ \mathrm{OPE}} \begin{cases} 1 & \text{if} \quad (X_a \wedge X_3)\cdot(X_4 \wedge X_5) > 0\,, \\ 0 & \text{else}\,, \end{cases} \tag{3.20}$$

while the cross ratios z_2, $\bar{z}_2$ and Υ all tend to zero. On the other hand, if we were to take the limit from the right side in the $((65)4)$ order, we would end up with

$$w_2 \xrightarrow{((65)4)\ \mathrm{OPE}} \begin{cases} 1 & \text{if} \quad (X_2 \wedge X_3)\cdot(X_4 \wedge X_c) > 0\,, \\ 0 & \text{else}\,, \end{cases} \tag{3.21}$$

while, once again, $z_2, \bar{z}_2$ and Υ vanish in the limit. This instructs us on the fact that the relevant regime to study the projection on exchanges of specific operators in the leg b of the six-point function is the part that is common to both OPE limits taken above, namely $(z_2, \bar{z}_2, \Upsilon) \to 0$. Taking only these three cross ratios to zero, while leaving all others finite, corresponds to a regime in which the two triples (x_1, x_2, x_3) and (x_4, x_5, x_6) can each be enclosed in a sphere of radius r which is parametrically smaller than the distance R between any two points of the two triples. In this limiting regime, we need the six remaining cross ratios to parameterise the configuration of points in the two small spheres, see appendix C for some more details.

3.3 OPE limits of six-point blocks

Our main goal in this subsection is to analyse the asymptotics of the six-point comb channel blocks in the limit where we send $\bar{z}_2, z_2$ and Υ to zero. We will first study the limiting

JHEP06(2022)144

behaviour of the Casimir equation for $\mathcal{D}^2_{(123)}$ under the assumption that eigenfunctions obey a leading power law behaviour

$$\Psi(z_s, \bar{z}_s, w_r, \Upsilon) \sim \bar{z}_2^{p_1} z_2^{p_2} \Upsilon^{p_3} \left(\psi(z_1, \bar{z}_1, z_3, \bar{z}_3, w_1, w_2) + O(z_2, \bar{z}_2, \Upsilon)\right) \tag{3.22}$$

in the three variables for the middle leg. Similarly to exchanges of STTs, see our review in subsection 3.1, the precise powers depend on the order in which the limits are taken. Taking the limit $\Upsilon \to 0$ first turns out to be inconsistent, as it produces divergences in the Casimir equation. Instead, we first take the $\bar{z}_2 \to 0$ limit followed by the one in z_2, in direct analogy to the $N = 4, 5$-point functions. Alternatively, we could also send z_2 to zero first, but this is a mere issue of convention given the symmetry of the cross ratios under $z \leftrightarrow \bar{z}$ and $w \leftrightarrow (1 - w)$. Once this limit is performed, the order of the remaining two limits is irrelevant and one finds

$$\bar{z}_2^{-p_1} z_2^{-p_2} \Upsilon^{-p_3} \mathcal{D}^2_{(123)} \bar{z}_2^{p_1} z_2^{p_2} \Upsilon^{p_3} \underset{z_2, \Upsilon \to 0}{\overset{\bar{z}_2 \to 0}{\longrightarrow}} -2\Big(d\, p_1 - p_1^2 - p_2^2 + (p_3+1)(p_2 - p_1) - p_3(p_3 - 1)\Big) + \ldots, \tag{3.23}$$

where we indicated the order of limits by placing the first one above the arrow and the remaining two below. As before, the ... correspond to higher order terms in $z_2, \bar{z}_2$ and Υ. This behaviour, in which the leading term of the second order Casimir differential operator for the central link is a constant, was what we were aiming for when we introduced the OPE coordinates.

Of course, the constant term must be equal to the eigenvalue of the quadratic Casimir element in the MST_2 representation of the exchanged intermediate field. The latter is related to the weight and spin labels of said fields as

$$C^2(\Delta_b, l_b, \ell_b) = \Delta_b(\Delta_b - d) + l_b(l_b + d - 2) + \ell_b(\ell_b + d - 4)\,. \tag{3.24}$$

Equating this with eq. (3.23), we can only match the coefficients in front of the dimension d provided that

$$p_1 = \frac{\Delta_b - l_b - \ell_b}{2}\,.$$

Then to ensure that Ψ is single-valued in the $(z_2, \bar{z}_2)$ plane, we must set the exponent p_2 of the variable z_2 to be

$$p_2 = \frac{\Delta_b + l_b + \ell_b}{2}\,. \tag{3.25}$$

This also ensures that for $\ell_b = 0$, one recovers the usual leading behaviour for intermediate STT exchange, see subsection 3.1. Requiring finally a full match with the Casimir eigenvalue leaves us with two possible solutions for the leading behaviour in Υ

$$p_3 = \ell_b \qquad \text{or} \qquad p_3 = l_b + 1\,. \tag{3.26}$$

This freedom, which cannot be eliminated by considering higher Casimir differential operators, is associated with the invariance of the Casimir elements under the action of Weyl transformations. Let us note that the two possible solutions correspond to the two possible

JHEP06(2022)144

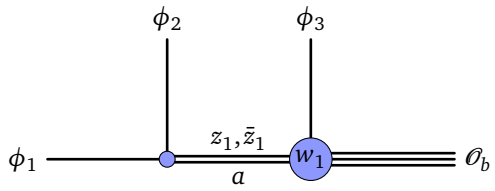

Figure 6: One of the four-point functions obtained in the OPE limit for the middle leg in a six-point function in comb channel. The rightmost field is a Mixed-Symmetry Tensor with two spin indices and the exchanged field is a Symmetric Traceless Tensor.

behaviours in $(1-v)$ for the four-point s-channel OPE that distinguish between Euclidean and Minkowski conformal blocks [44],

$$(1-v)^{l}\,, \qquad \text{or} \qquad (1-v)^{1-\Delta}\,, \tag{3.27}$$

modulo an exchange of $-\Delta \leftrightarrow l$ and $l \leftrightarrow \ell$. Following the interpretation of Υ as a degree of freedom associated with MST_2 fields, the first solution with $p_3 = \ell_b$ is the most natural. This choice will later be validated when we compare the limiting behaviour of the remaining non-trivial Casimir operators to those of spinning four-point blocks.

Now let us address the second part of our claim. As stated in the introduction, we want to show that expansion of the conformal block (3.22) takes the more specific form

$$\Psi(z_r, \bar{z}_r, w_1, w_2, \Upsilon) \overset{\bar{z}_2, z_2, \Upsilon \to 0}{\sim} \bar{z}_2^{\frac{\Delta_b - l_b - \ell_b}{2}} z_2^{\frac{\Delta_b + l_b + \ell_b}{2}} \Upsilon^{\ell_b} \left(\psi_a(z_1, \bar{z}_1, w_1)\psi_c(z_3, \bar{z}_3, w_2) + \dots\right)\,, \tag{3.28}$$

in which the leading term splits into a product of two functions of three variables each. Furthermore, we want to prove that each of these two factors is a spinning four-point conformal block, one corresponding to the left side of the OPE diagram, see figure 6, the other for the right. The proof is a nice application of Gaudin integrability, i.e. our characterisation of multipoint conformal blocks through differential equations. Having seen that the differential operators $\mathcal{D}^p_{(123)}, p = 2, 3, 4$, simply act as multiplication with the value of the associated Casimir elements, we now need to study the limiting behaviour of the remaining six differential operators. These include two quadratic and two fourth order Casimir operators, as well as two vertex operators. We will focus our discussion on the quadratic Casimir operators. Crucially, we find that the two quadratic Casimirs $\mathcal{D}^2_{(12)}$ and $\mathcal{D}^2_{(56)}$ decouple completely upon taking the OPE limit in the central link,

$$\mathcal{D}^2_{(12)} \xrightarrow{b\,\text{OPE}} \mathcal{D}^2_a(z_1, \bar{z}_1, w_1)\,, \qquad \mathcal{D}^2_{(123)} \xrightarrow{b\,\text{OPE}} C^2(\Delta_b, l_b, \ell_b)\,, \qquad \mathcal{D}^2_{(56)} \xrightarrow{b\,\text{OPE}} \mathcal{D}^2_c(z_3, \bar{z}_3, w_2)\,. \tag{3.29}$$

Here, b OPE denotes the limit in which we take $\bar{z}_2$ to zero followed by z_2 and Υ, as discussed

before. It suffices to spell out an expression for $\mathcal{D}_a^2$, which takes the relatively simple form

$$\begin{aligned}\mathcal{D}_a^2 = &-2(z_1-1)z_1^2\partial_{z_1}^2 - 2(\bar{z}_1-1)\bar{z}_1^2\partial_{\bar{z}_1}^2 + \frac{4(w_1-1)w_1z_1\bar{z}_1(w_1(z_1-\bar{z}_1)+\bar{z}_1-1)}{(z_1-\bar{z}_1)^2}\partial_{w_1}^2 \\ &+2(1-w_1)w_1z_1^2\partial_{z_1}\partial_{w_1} - 2(1-w_1)w_1\bar{z}_1^2\partial_{\bar{z}_1}\partial_{w_1} \\ &+2\left[z_1^2\left(a+b-1+\left(w_1-\frac{1}{2}\right)l_b\right)+\frac{z_1\bar{z}_1}{z_1-\bar{z}_1}(1-z_1)(d-2)\right]\partial_{z_1} \\ &+2\left[\bar{z}_1^2\left(a+b-1-\left(w_1-\frac{1}{2}\right)l_b\right)-\frac{z_1\bar{z}_1}{z_1-\bar{z}_1}(1-\bar{z}_1)(d-2)\right]\partial_{\bar{z}_1} \\ &+2\Bigg[a(w_1-1)w_1(z_1-\bar{z}_1)-\frac{2(w_1-1)w_1z_1\bar{z}_1(l_b-1)}{z_1-\bar{z}_1} \\ &\quad+\frac{z_1\bar{z}_1(d-2)(w_1(\bar{z}_1+z_1-2)-\bar{z}_1+1)}{(z_1-\bar{z}_1)^2}\Bigg]\partial_{w_1} \\ &-a[(2w_1-1)(z_1-\bar{z}_1)l_b+2b(\bar{z}_1+z_1)]-\frac{z_1\bar{z}_1(w_1(z_1-\bar{z}_1)+\bar{z}_1-1)}{(w_1-1)w_1(z_1-\bar{z}_1)^2}\ell_b(\ell_b+d-4)\,,\end{aligned} \tag{3.30}$$

where the constants a, b are determined by the conformal weights of the external scalars and Δ_b through $2a = \Delta_2 - \Delta_1$ and $2b = \Delta_3 - \Delta_b$. Then the expression for $\mathcal{D}_c^2$ is the same, but with variables $z_3, \bar{z}_3, w_2$ instead of $z_1, \bar{z}_2, w_1$, along with the parameters $2a = \Delta_4 - \Delta_b$ and $2b = \Delta_3 - \Delta_4$. We have also analysed the fourth order Casimir operators, as well as the vertex operators, and have found that they display the same decoupling. We refrain from spelling out explicit expressions here.

For the time being, all we can do with the explicit expression for $\mathcal{D}_a^2$ is appreciate that the formula looks relatively simple. In the next section, we will analyse it further and show that it can be mapped to the quadratic Casimir operator for a spinning four-point function with three scalar and one MST_2 external field. Let us note that the blocks for such spinning four-point functions indeed depend on three variables, the two 4-point cross ratios and one additional variable associated with the choice of tensor structure at the scalar-STT-MST_2 vertex. In particular, our analysis implies that conformal partial waves in this limit are polynomials of a bounded degree in a variable closely related to w_1, given in (4.40), a fact that is already non-trivial from the mere definition of OPE cross ratios.

Before concluding this section, we briefly want to discuss a second OPE limit that we have also worked out explicitly. It concerns a setup where two OPE limits are taken on the links a and c, leaving a four-point function of two STT fields and two scalars, see figure 7. We perform this limit by first sending $\bar{z}_1$ and $\bar{z}_2$ to zero before taking the limits $z_1, z_2 \to 0$. In this limit, five of the nine cross ratios survive and one finds

$$\psi(z_1,\bar{z}_1,z_2,\bar{z}_2,z_3,\bar{z}_3,w_1,w_2,\Upsilon) \overset{\bar{z}_1,z_1,\bar{z}_3,z_3\to 0}{\sim} \bar{z}_1^{\frac{\Delta_a-l_a}{2}} z_1^{\frac{\Delta_a+l_a}{2}} \bar{z}_3^{\frac{\Delta_c-l_c}{2}} z_3^{\frac{\Delta_c+l_c}{2}} (\psi_b(z_2,\bar{z}_2,w_1,w_2,\Upsilon)+\dots)\,. \tag{3.31}$$

JHEP06(2022)144

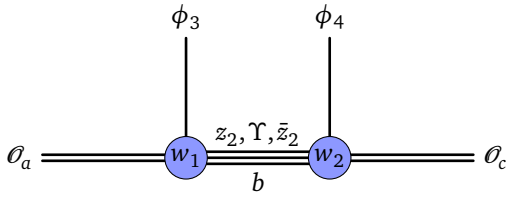

Figure 7: Four-point function obtained from OPE limit on legs a and c of a six-point function in comb channel. Fields at legs a and c are Symmetric Traceless Tensors, while the exchanged field is a Mixed-Symmetry Tensor with two spin indices.

The derivation of this limit follows the same steps we carried out in the discussion of the OPE limit on the link b above. In particular, upon taking the combined a and c OPE limit, one can show that the second order Casimir operators behave as

$$\mathcal{D}^2_{(12)}, \mathcal{D}^2_{(56)} \xrightarrow{(a+c)\,\text{OPE}} C^2(\Delta_a, l_c), C^2(\Delta_c, l_c)\,, \qquad \mathcal{D}^2_{(123)} \xrightarrow{(a+c)\,\text{OPE}} \mathcal{D}^2_b(z_2, \bar{z}_2, w_1, w_2, \Upsilon)\,. \tag{3.32}$$

The second order Casimir element for the link b reduces to an operator in the five remaining variables that can be worked out explicitly, even though the expression is a bit longer than in our discussion above. It can be found in the Mathematica notebook we include with this publication. In the next section, we will show that this five-variable Casimir operator can be mapped to the Casimir operator of a spinning four-point function with two scalars and two STTs attached on either side of the OPE diagram.

4 Spinning Calogero-Sutherland models

In the last section, we computed the six-point comb channel Casimir differential equations in two OPE limits. In the first case, we performed the OPE limit on the central link of the OPE diagram and obtained two sets of Casimir operators that act on three cross ratios each. The second order Casimir operators were spelled out in eq. (3.30). The second setup involved a combined OPE limit on the left and the right link, resulting in a set of Casimir operators acting on a five-variable system. In both cases, the reduced system should correspond to a spinning four-point correlator, involving either three scalars and one MST, or two scalars and two STT external fields. The Casimir operators for such four-point blocks have been constructed in some examples, see e.g. [9, 39, 40, 45]. Here we shall report on a very recent observation that all of these Casimir operators can be constructed from Harish-Chandra's radial component map [43]. In fact, the construction works for arbitrary spinning four-point functions in any dimension.

We shall provide a short review of previous work on the relation between spinning conformal blocks and harmonic analysis of spherical functions in the first subsection before spelling out the universal spinning Casimir operators in the second. The general construction will be worked out explicitly in a number of examples, including the two cases we mentioned in the previous paragraph. In the third subsection, we then construct an explicit map between the OPE limits of Casimir operators obtained in the previous section

JHEP06(2022)144

and spinning four-point Casimir operators, thereby proving the claim that e.g. the Casimir operator in eq. (3.30) is identical to the Casimir operator for a spinning four-point function.

4.1 Spherical functions and the radial part of the Laplacian

As was shown in [39, 40, 46], conformal four-point functions admit a realisation as covariant vector-valued functions on the conformal group $G \sim \mathrm{SO}(d+1,1)$,[5] itself. More precisely, there is a bijective correspondence between solutions to conformal Ward identities and K-spherical functions on G, where $K \sim \mathrm{SO}(1,1) \times \mathrm{SO}(d)$ is the group of rotations and dilations. Given two finite-dimensional irreducible representations ρ_L and ρ_R of K, with carrier spaces $W_{L,R}$, the space of K-spherical functions is defined as

$$\Gamma_{\rho_L,\rho_R} = \{f : G \to \mathrm{Hom}(W_R, W_L) \mid f(k_L g k_R) = \rho_L(k_L) f(g) \rho_R(k_R)\}, \quad g \in G,\ k_{L,R} \in K\,. \tag{4.1}$$

We may, and occasionally will, identify $\mathrm{Hom}(W_R, W_L) \cong W_L \otimes W_R^*$. Covariance properties of f are then written as

$$f\left(k_L g k_R\right) = \left(\rho_L\left(k_L\right) \otimes \rho_R^*\left(k_R^{-1}\right)\right) f(g)\,. \tag{4.2}$$

The explicit map between K-spherical functions and conformal correlators may be found in [41, 47].

By reinterpreting conformal correlators as K-spherical functions on the conformal group, conformal blocks are carried to eigenfunctions of the group Laplacian, thus becoming a subject of harmonic analysis. By definition, spherical harmonics are eigenfunctions of the *radial part* of the Laplacian. The latter may be thought of as a differential operator in two variables with matrix coefficients. To explain this, we recall that the conformal group G admits a Cartan decomposition

$$G = K A_p K\,. \tag{4.3}$$

In other words, almost every[6] element of G can be factorised as $g = k_L a k_R$, with $k_L, k_R \in K$ and $a \in A_p$. The factor A_p is the two-dimensional abelian group generated by elements $H_1 = \frac{1}{2}(P_1 + K_1)$ and $H_2 = -\frac{i}{2}(P_2 - K_2)$, where P_μ, K_μ denote generators of translations and special conformal transformations, respectively. Clearly, spherical functions are uniquely determined by their restrictions to A_p. Furthermore, such restrictions are not arbitrary. Let $M \sim \mathrm{SO}(d-2)$ be the centraliser of A_p in K. For any $m \in M$, given one decomposition $g = k_L a k_R$, we can form another $g = (k_L m) a (m^{-1} k_R)$ (one can fix the ambiguity by requiring that either k_L or k_R belongs to a particular section of K/M). When restricted to A_p, spherical functions take values in the space of M-invariants inside $\mathrm{Hom}(W_R, W_L)$. Indeed,

$$f(a) = f(mam^{-1}) = \rho_L(m) f(a) \rho_R(m^{-1})\,. \tag{4.4}$$

Because it commutes with left and right regular representations, the Laplacian Δ preserves the space Γ_{ρ_L,ρ_R}. The above comments allow us to regard its restriction to this space as a differential operator that acts on vector-valued functions in two variables.

[5] We write $G \sim H$ to mean that Lie groups G and H are locally isomorphic, i.e. $Lie(G) \cong Lie(H)$.

[6] The set of elements that cannot be factorised has Haar measure zero.

JHEP06(2022)144

4.2 Spinning blocks and Calogero-Sutherland models

We will now explain how radial parts of the Laplacian are related to spinning Calogero-Sutherland models.

Let $h = \exp(t_1 H_1 + t_2 H_2)$ be an element of A_p and write $X' = h^{-1} X h$ for any $X \in \mathfrak{g}$.[7] The quadratic Casimir of $\mathfrak{g}$ can be written as

$$\begin{aligned} C_2 = {} & H_1^2 + H_2^2 + \coth(t_1+t_2)(H_1+H_2) + \coth(t_1-t_2)(H_1-H_2) \\ & + (d-2)\left(\coth t_1 H_1 + \coth t_2 H_2\right) \\ & - \frac{D_+'^2 - 2\cosh(t_1+t_2) D_+' D_+ + D_+^2}{2\sinh^2(t_1+t_2)} - \frac{D_-'^2 - 2\cosh(t_1-t_2) D_-' D_- + D_-^2}{2\sinh^2(t_1-t_2)} \\ & + \sum_{a=3}^{d} \left(\frac{M_{1a}'^2 - 2\cosh t_1 M_{1a}' M_{1a} + M_{1a}^2}{\sinh^2 t_1} + \frac{M_{2a}'^2 - 2\cosh t_2 M_{2a}' M_{2a} + M_{2a}^2}{\sinh^2 t_2} \right) - \frac{1}{2} M^{ab} M_{ab}, \end{aligned} \tag{4.5}$$

where we have introduced $D_\pm = D \pm \mathrm{i} M_{12}$ and indices a, b to run over the set $\{3, 4, \ldots, d\}$. In the remainder of this section, Latin indices will always be assumed to be in this range. The validity of the last equation can be readily checked and we provide a short derivation in appendix A. We call the above equation the radial decomposition of C_2. More generally, the radial decomposition of elements in $\mathrm{U}(\mathfrak{g}_c)$ may be thought of as an infinitesimal version of the Cartan decomposition. The significance of the radial decomposition of C_2 lies in the fact that it allows to directly reduce the Laplacian to any space of K-spherical functions. All one needs to do is substitute the generators H_i by partial derivatives ∂_{t_i}, the primed generators x', with $x \in \mathfrak{k}_c$, by representation operators $\rho_L(x)$, and the unprimed generators $y \in \mathfrak{k}_c$ by $\rho_R^*(-y)$. The fact that the same prescription can be applied for all choices of ρ_L and ρ_R is captured by a universal map

$$\Pi : \mathrm{U}(\mathfrak{g}_c) \to \mathcal{D}(A_p) \otimes \left(\mathrm{U}(\mathfrak{k}_c) \otimes_{\mathrm{U}(\mathfrak{m}_c)} \mathrm{U}(\mathfrak{k}_c) \right), \tag{4.6}$$

which assigns to any element of $\mathrm{U}(\mathfrak{g}_c)$ a (class of a) differential operator on A_p with coefficients in two copies of $\mathrm{U}(\mathfrak{k}_c)$ (here $\mathcal{D}(A_p)$ denotes the algebra of differential operators on A_p). The latter is called Harish-Chandra's radial component map. In practice, for any $u \in \mathrm{U}(\mathfrak{g}_c)$, $\Pi(u)$ is computed by radially decomposing u,[8] and then replacing elements x', with $x \in \mathrm{U}(\mathfrak{k}_c)$, by $x \otimes 1$ and elements y, with $y \in \mathfrak{k}_c$, by $1 \otimes y$. The replacements here belong to the product of two *commuting* copies of $\mathrm{U}(\mathfrak{k}_c)$.

[7] We use the notation $\mathfrak{g} = Lie(G)$ and $\mathfrak{g}_c = \mathfrak{g} \otimes \mathbb{C}$ and similarly for Lie algebras of all other groups under consideration.

[8] Almost any element $h \in A_p$ provides an isomorphism of vector spaces $\mathrm{U}(\mathfrak{g}_c) \cong \mathrm{U}(\mathfrak{a}_{p_c}) \otimes (\mathrm{U}(\mathfrak{k}_c) \otimes_{\mathrm{U}(\mathfrak{m}_c)} \mathrm{U}(\mathfrak{k}_c))$

$$\Gamma_h : \mathrm{U}(\mathfrak{a}_{p_c}) \otimes \mathrm{U}(\mathfrak{k}_c) \otimes \mathrm{U}(\mathfrak{k}_c) \to \mathrm{U}(\mathfrak{g}_c), \quad \Gamma_h(H \otimes x \otimes y) = h^{-1} x h \; H \; y \,.$$

The element of $\mathrm{U}(\mathfrak{g}_c)$ on the right hand side is said to be in a radially-decomposed form with respect to h. Notice that $\mathrm{U}(\mathfrak{a}_{p_c})$ is naturally represented by differential operators on A_p with constant coefficients, i.e. $\mathrm{U}(\mathfrak{a}_{p_c}) \cong \mathbb{C}[\partial_{t_1}, \partial_{t_2}]$.

The universal Calogero-Sutherland Hamiltonian is a close cousin of the universal radial part of the Laplacian $\Pi(C_2)$ (see [48, 49] for a recent discussion). The two are related by conjugation, $H = \delta\Pi(C_2)\delta^{-1}$, with respect to the factor

$$\delta(t_i) = \sqrt{\sinh^{d-2} t_1 \sinh^{d-2} t_2 \sinh(t_1+t_2)\sinh(t_1-t_2)}\,. \tag{4.7}$$

This is the essentially unique factor that gives an operator in a Schrödinger form, i.e. without first order derivatives in t_i. Explicitly, the universal Hamiltonian reads

$$\begin{aligned} H = {} & \partial_{t_1}^2 + \partial_{t_2}^2 + \frac{1 - D_+'^2 + 2\cosh(t_1+t_2) D_+' D_+ - D_+^2}{2\sinh^2(t_1+t_2)} \\ & + \frac{1 - D_-'^2 + 2\cosh(t_1-t_2) D_-' D_- - D_-^2}{2\sinh^2(t_1-t_2)} \\ & + \frac{M_{1a}' M_{1a}' - 2\cosh t_1 M_{1a}' M_{1a} + M_{1a} M_{1a} - \frac{1}{4}(d-2)(d-4)}{\sinh^2 t_1} \\ & + \frac{M_{2a}' M_{2a}' - 2\cosh t_2 M_{2a}' M_{2a} + M_{2a} M_{2a} - \frac{1}{4}(d-2)(d-4)}{\sinh^2 t_2} \\ & - \frac{1}{2} M^{ab} M_{ab} - \frac{d^2-2d+2}{2}\,. \end{aligned} \tag{4.8}$$

We have slightly abused the notation here: in eq. (4.5), both M_{1a} and M_{1a}' are elements of $\mathrm{U}(\mathfrak{g}_c)$ and $M_{1a}' = h^{-1} M_{1a} h$, whereas in eq. (4.8), they are elements of $\mathrm{U}(\mathfrak{k}_c) \otimes \mathrm{U}(\mathfrak{k}_c)$. Spinning Calogero-Sutherland Hamiltonians H_{ρ_L,ρ_R} are obtained from H by substituting $x' \to \rho_L(x)$ and $y \to \rho_R^*(-y)$, with $x, y \in \mathrm{U}(\mathfrak{k}_c)$, in accordance with the prescription spelled out above. Equation (4.8) is the main result of this section and all applications below emerge from its special cases. Compared to the previous works [39, 40], which computed H_{ρ_L,ρ_R} for some particular representations $\rho_{L,R}$, the new observation of [43] concerns the universal spin dependence of these Schrödinger operators.[9]

As a first simple illustration of this universal formula let us briefly discuss the case of scalar functions on G. These correspond to four-point functions of scalar fields. For K-K invariant functions, i.e. trivial representations $\rho_L = \rho_R = 1$ the Hamiltonian we get reads

$$\begin{aligned} H_0 = {} & \partial_{t_1}^2 + \partial_{t_2}^2 + \frac{1}{2}\left(\frac{1}{\sinh^2(t_1+t_2)} + \frac{1}{\sinh^2(t_1-t_2)}\right) \\ & - \frac{(d-2)(d-4)}{4}\left(\frac{1}{\sinh^2 t_1} + \frac{1}{\sinh^2 t_2}\right) - \frac{d^2-2d+2}{2}\,. \end{aligned}$$

To make our coordinates on A_p agree with [39, 40], we introduce $u_1 = t_1 + t_2$ and $u_2 = t_1 - t_2$.

[9] In the most direct way to derive Casimir equations for spinning conformal blocks, one would introduce spin by modifying generators of conformal transformations that act on individual fields. Upon reduction to the cross ratio space, this produces additional terms in the Casimir operator. Our procedure circumvents the reduction of spinning degrees of freedom and adds their contribution to the reduced operator directly.

JHEP06(2022)144

The Hamiltonian then can be written as

$$H_0 = -2\left(H_{PT}^{(0,0)}(u_1) + H_{PT}^{(0,0)}(u_2) + \frac{(d-2)(d-4)}{8}\left(\frac{1}{\sinh^2\frac{u_1+u_2}{2}} + \frac{1}{\sinh^2\frac{u_1-u_2}{2}}\right)\right) - \frac{d^2-2d+2}{2}, \tag{4.9}$$

where $H_{PT}^{(a,b)}$ denotes the quantum mechanical Pöschl-Teller Schrödinger operator.[10] The H_0 is the Hamiltonian of the hyperbolic BC_2 Calogero-Sutherland model with parameters $a = 0$, $b = 0$ and $\epsilon = d - 2$, justifying our terminology. More precisely

$$H_0 = -2H_{cs}^{(0,0,d-2)} - \frac{d^2-2d+2}{2}. \tag{4.10}$$

For non-identical scalar fields, ρ_L and ρ_R are characters of the dilation group $\mathrm{SO}(1,1)$ and trivial representations of $\mathrm{SO}(d)$. Writing $\rho_L(D) = 2a$ and $\rho_R^*(D) = 2b$, we obtain the potential

$$V_{\rho_L,\rho_R} = -\frac{2a^2 - 4\cosh(t_1+t_2)ab + 2b^2}{\sinh^2(t_1+t_2)} - \frac{2a^2 - 4\cosh(t_1-t_2)ab + 2b^2}{\sinh^2(t_1-t_2)}. \tag{4.11}$$

Then the full Hamiltonian is that of the BC_2 Calogero-Sutherland model with parameters a, b and $\epsilon = d - 2$,

$$H_{\rho_L,\rho_R} = H_0 + V_{\rho_L,\rho_R} = -2H_{cs}^{(a,b,d-2)} - \frac{d^2-2d+2}{2}. \tag{4.12}$$

Wave functions of this operator were constructed in the seminal work of Heckman and Opdam [37]. Finally, assume ρ_L and ρ_R to be arbitrary finite-dimensional representations. Due to the invariance condition (4.4), the Hamiltonian H_{ρ_L,ρ_R} is restricted to act on functions $F : A_p \to W_L \otimes W_R^*$ that satisfy $(\rho_L(M_{ab}) + \rho_R^*(M_{ab}))F = 0$. It is not difficult to see from the expression (4.8) that H_{ρ_L,ρ_R} is indeed a well-defined operator on this space. By writing $\rho_L(x)$ and $\rho_R^*(-y)$ as matrices, one ends up with a certain matrix Schrödinger operator. Here we will follow a slightly different path: representations ρ_L and ρ_R of $\mathfrak{k}_c$ will be written in terms of differential operators that act on finite-dimensional spaces of polynomials. This allows for an elegant implementation of the M-invariance conditions — the "spin cross ratios" of previous sections will arise as generators of M-invariants in $\mathrm{Hom}(W_R, W_L)$. When prepared in this way, the spinning Hamiltonians may be compared to those obtained through the OPE limit construction.

We will consider two examples in particular: 1) the representation ρ_L is trivial and ρ_R is a mixed symmetry tensor of depth two, or 2) both ρ_L and ρ_R are symmetric traceless tensors. Here, we are referring to the $\mathrm{SO}(d)$ content of these representations. By the dictionary of [39, 41], the two cases correspond in conformal field theory to a four-point function of an MST_2 field and three scalars, or two STTs and two scalars, respectively. These examples therefore describe the two OPE limits analysed in the previous section.

[10] Conventions for Pöschl-Teller and Calogero-Sutherland Hamiltonians $H_{PT}^{(a,b)}$, $H_{cs}^{(a,b,\epsilon)}$ are the same as in [50].

JHEP06(2022)144

4.2.1 One $\mathbf{MST_2}$ and three scalars

We consider spinning Calogero-Sutherland Hamiltonians that arise when one of the representations ρ_L, ρ_R is trivial. For concreteness, let ρ_L be the trivial representation. The potential in the Schrödinger operator the simplifies to

$$V = -\frac{D_+^2}{2\sinh^2(t_1+t_2)} - \frac{D_-^2}{2\sinh^2(t_1-t_2)} + \sum_{a=3}^{d}\left(\frac{M_{1a}^2}{\sinh^2 t_1} + \frac{M_{2a}^2}{\sinh^2 t_2}\right) - \frac{1}{2}M^{ab}M_{ab}\,. \tag{4.13}$$

We assume that ρ_R is a mixed symmetry tensor (l,ℓ) of depth two of the rotation group. Thus, the generators may be realised as differential operators

$$\mathrm{i}M_{12} \to \rho_R^*(-\mathrm{i}M_{12}) = z^a\partial_a - l, \quad M_{ab} \to z_b\partial_{z^a} - z_a\partial_{z^b} + w_b\partial_{w^a} - w_a\partial_{w^b}, \tag{4.14}$$

$$\mathrm{i}M_{1a} \to \frac{1}{2}\left(\left(1+z^2\right)\partial_{z^a} - 2z_a\left(z^b\partial_{z^b} - l\right) + 2z^b\left(w_b\partial_{w^a} - w_a\partial_{w^b}\right)\right), \tag{4.15}$$

$$M_{2a} \to \frac{1}{2}\left(\left(1-z^2\right)\partial_{z^a} + 2z_a\left(z^b\partial_{z^b} - l\right) - 2z^b\left(w_b\partial_{w^a} - w_a\partial_{w^b}\right)\right), \tag{4.16}$$

acting on polynomial functions of z^a and w^a. In the following, to simplify notation, we will write the differential operators $\rho_R^*(-M_{ab})$ simply as M_{ab}. The invariance condition (4.4) reads $M_{ab}f = 0$ and is solved by functions of the variables

$$X = z^a z_a, \qquad W = w^a w_a, \qquad Y = z^a w_a\,. \tag{4.17}$$

To get to the carrier space of ρ_R^*, we are further required to impose the homogeneity $Y\partial_Y f = \ell f$ and restrict to the lightcone $\{W = 0\}$. Individual pieces of the Hamiltonian (4.8) restrict to well-defined operators on such functions. Introducing the operator

$$\begin{aligned} L_{l,\ell}(X) = &-X(1-X)^2\partial_X^2 - \left(\ell(1-X) - 2(1-l)X + \frac{d-2}{2}(1+X)\right)(1-X)\partial_X \\ &+ \left(1-l-\frac{d-2}{2}\right)(\ell(1-X) + lX) - \frac{l(d-2)}{2}, \end{aligned} \tag{4.18}$$

we have

$$D = 2b, \qquad \mathrm{i}M_{12} = 2X\partial_X + \ell - l, \qquad M_{1a}M_{1a} = L(X), \qquad M_{2a}M_{2a} = L(-X)\,. \tag{4.19}$$

Therefore, the Hamiltonian reads

$$\begin{aligned} H_{l,\ell}^{(b)} = &\partial_{t_1}^2 + \partial_{t_2}^2 + \frac{1-(2b+\ell-l+2X\partial_X)^2}{2\sinh^2(t_1+t_2)} + \frac{1-(2b-\ell+l-2X\partial_X)^2}{2\sinh^2(t_1-t_2)} \\ &+ \frac{L_{l,\ell}(X) - \frac{1}{4}(d-2)(d-4)}{\sinh^2 t_1} + \frac{L_{l,\ell}(-X) - \frac{1}{4}(d-2)(d-4)}{\sinh^2 t_2} - \frac{d^2-2d+2}{2}\,. \end{aligned} \tag{4.20}$$

Note that the Hamiltonian acts on three variables, t_1, t_2 and X. We will compare it to the second order differential operator (3.30), obtained in the previous section from the OPE limit at the central intermediate link of the six-point function.

JHEP06(2022)144

4.2.2 Two STTs and two scalars

Let us now address the second case, in which the left and right representations of the rotation group are both symmetric traceless tensors. This leads to the Calogero-Sutherland Hamiltonian as a differential operator in five variables. In the universal Calogero-Sutherland Hamiltonian, we are required to make substitutions

$$\mathrm{i}M'_{12} \to \rho_L(\mathrm{i}M_{12}) = -z'^a\partial'_a + l', \quad M'_{ab} \to z'_a\partial'_b - z'_b\partial'_a, \tag{4.21}$$

$$\mathrm{i}M'_{1a} \to -\frac{1}{2}\left((1+z'^2)\partial'_a - 2z'_a(z'^b\partial'_b - l')\right), \quad M'_{2a} \to -\frac{1}{2}\left((1-z'^2)\partial'_a + 2z'_a(z'^b\partial'_b - l')\right), \tag{4.22}$$

$$\mathrm{i}M_{12} \to \rho^*_R(-\mathrm{i}M_{12}) = z^a\partial_a - l, \quad M_{ab} \to z_b\partial_a - z_a\partial_b, \tag{4.23}$$

$$\mathrm{i}M_{1a} \to \frac{1}{2}\left((1+z^2)\partial_a - 2z_a(z^b\partial_b - l)\right), \quad M_{2a} \to \frac{1}{2}\left((1-z^2)\partial_a + 2z_a(z^b\partial_b - l)\right). \tag{4.24}$$

The invariance condition $(M'_{ab} - M_{ab})f = 0$ then means that f depends only on the scalar products

$$X_R = z^a z_a, \qquad X_L = z'^a z'_a, \qquad Y = z^a z'_a\,. \tag{4.25}$$

Individual pieces of the Hamiltonian commute with the constraints, so they reduce to operators in the variables (X_R, X_L, Y). To write them down, we introduce

$$\begin{aligned}
&L_1(X_R,X_L,Y)\\
&=\frac{1}{4}\Big(-4X_R(1-X_R)^2\partial^2_{X_R} - 4Y(1-X_R)^2\partial_{X_R}\partial_Y + \left(4Y^2-(1+X_R)^2X_L\right)\partial^2_Y\\
&\quad +2(1-X_R)(4(1-l)X_R-(d-2)(1+X_R))\partial_{X_R}\\
&\quad -2Y((-2l-d+4)X_R+2l-d+2)\partial_Y + 2l(2(1-l)X_R-(d-2)(1+X_R))\Big),
\end{aligned} \tag{4.26}$$

and

$$\begin{aligned}
&L_2(X_R,X_L,Y)\\
&=-\frac{1}{4}\Big(-4Y(1-X_R)(1-X_L)\partial_{X_R}\partial_{X_L} - 2(1-X_R)\left(X_R(1+X_L)-2Y^2\right)\partial_{X_R}\partial_Y\\
&\quad -2(1-X_L)\left(X_L(1+X_R)-2Y^2\right)\partial_{X_L}\partial_Y + \left(-4Y^3+Y(-1+X_R+X_L+3X_RX_L)\right)\partial^2_Y\\
&\quad +\Big((2-d)(1+X_R)(1+X_L)+2(1-l)X_R(1+X_L)+2(1-l')X_L(1+X_R)\\
&\qquad -4(1-l-l')Y^2\Big)\partial_Y\\
&\quad -4lY(1-X_L)\partial_{X_L} - 4l'Y(1-X_R)\partial_{X_R} - 4ll'Y\Big).
\end{aligned} \tag{4.27}$$

Then we have

$$M_{1a}M_{1a} = L_1(X_R, X_L, Y), \qquad M_{2a}M_{2a} = L_1(-X_R, -X_L, -Y), \tag{4.28}$$

$$M'_{1a}M_{1a} = L_2(X_R, X_L, Y), \qquad M'_{2a}M_{2a} = L_2(-X_R, -X_L, -Y)\,. \tag{4.29}$$

Clearly, the operators $M'_{1a}M'_{1a}$ and $M'_{2a}M'_{2a}$ are obtained from $M_{1a}M_{1a}$ and $M_{2a}M_{2a}$ by exchanging X_R and X_L. Together with

$$\mathrm{i}M_{12} = 2X\partial_{X_R} + Y\partial_Y - l, \qquad \mathrm{i}M'_{12} = -2X_L\partial_{X_L} - Y\partial_Y + l', \tag{4.30}$$

$$\frac{1}{2}M^{ab}M_{ab} = \left(X_R X_L - Y^2\right)\partial_Y^2 - (d-3)Y\partial_Y\,, \tag{4.31}$$

these expressions are substituted in the formula (4.8) for the universal Hamiltonian to give the appropriate Calogero-Sutherland model that characterises four-point blocks with two scalars and two STTs. It will be compared with the Hamiltonian obtained from the double sided OPE limit of the six-point function in the previous section.

4.3 Mapping between OPE-reduced operators and Calogero-Sutherland form

Using the leading behaviours of six-point blocks spelled out in section 3 for various OPE limits, we will now recover the spinning four-point Casimir equations from the previous subsection. Our strategy is to map the differential equations we obtained when discussing OPE limits into the "standard form" of a quantum mechanical Hamiltonian, which can then be identified with one of the spinning Calogero-Sutherland Hamiltonians constructed above. As a rule of thumb, we will modify the second-order derivatives by performing a change of variables; all first-order derivatives can then be modified without affecting the second-order ones by "extracting" a certain function of the cross ratios from the target function. After this second operation, the new differential operator $\mathcal{D}'$ is related to the original one by conjugation with respect to the factor ω,

$$\psi = \omega\psi' \qquad \Longrightarrow \qquad \mathcal{D}' = \omega^{-1}\mathcal{D}\omega\,. \tag{4.32}$$

Let us now describe these steps in some more detail for the two cases analysed in the previous section.

4.3.1 One $\mathbf{MST_2}$ and three scalars

As a first step, we employ the change of variables used in [36],

$$z_1, \bar{z}_1 \qquad \longrightarrow \qquad \begin{cases} t_1 = \mathrm{i}\left[\arcsin\left(\frac{1}{\sqrt{z_1}}\right) + \arcsin\left(\frac{1}{\sqrt{\bar{z}_1}}\right)\right] \\ t_2 = \mathrm{i}\left[\arcsin\left(\frac{1}{\sqrt{z_1}}\right) - \arcsin\left(\frac{1}{\sqrt{\bar{z}_1}}\right)\right], \end{cases} \tag{4.33}$$

to map the second-order derivatives of $\mathcal{D}_a^2$ in z_1 and $\bar{z}_1$ to one-dimensional kinetic terms,

$$2z_1^2(1-z_1)\partial_{z_1}^2 + 2\bar{z}_1^2(1-\bar{z}_1)\partial_{z_1}^2 \qquad \longrightarrow \qquad \partial_{t_1}^2 + \partial_{t_2}^2\,. \tag{4.34}$$

JHEP06(2022)144

Secondly, we eliminate first order derivatives with respect to t_1 and t_2 via conjugation (4.32) by the factor

$$\omega(t_1,t_2,w_1) = (\sinh t_1 \sinh t_2)^{1-\frac{d}{2}} (\cosh t_1 - \cosh t_2)^{-a-b-\frac{1}{2}} (\cosh t_1 + \cosh t_2)^{a+b-\frac{1}{2}} \left(\frac{\sinh t_1 + \sinh t_2}{\sinh t_1 - \sinh t_2}(1-w_1)^2\right)^{\frac{l_b-\ell_b}{2}} . \tag{4.35}$$

We now wish to eliminate the mixed derivatives $\partial_{t_i}\partial_{w_1}$, thereby partially decoupling the internal leg and vertex degrees of freedom. This can be achieved by the change of variables

$$w_1 \qquad \longrightarrow \qquad X = \frac{\sinh t_1 - \sinh t_2}{\sinh t_1 + \sinh t_2}\frac{w_1}{1-w_1} . \tag{4.36}$$

The operator produced at the end of this procedure is in spinning Calogero-Sutherland form, and corresponds precisely to the operator spelled out in the previous subsection 4.2.1, see eq. (4.20).

4.3.2 Two STTs and two scalars

As in the previous subsection, the first step to map this operator to a quantum mechanical Hamiltonian is turning two derivatives into one-dimensional kinetic terms, which is done by transforming

$$z_2, \bar{z}_2 \qquad \longrightarrow \qquad \begin{cases} t_1 = \mathrm{i}\left[\arcsin\left(\frac{1}{\sqrt{z_2}}\right) + \arcsin\left(\frac{1}{\sqrt{\bar{z}_2}}\right)\right], \\ t_2 = \mathrm{i}\left[\arcsin\left(\frac{1}{\sqrt{z_2}}\right) - \arcsin\left(\frac{1}{\sqrt{\bar{z}_2}}\right)\right], \end{cases} \tag{4.37}$$

leading to

$$2z_2^2(1-z_2)\partial_{z_2}^2 + 2\bar{z}_2^2(1-\bar{z}_2)\partial_{z_2}^2 \qquad \longrightarrow \qquad \partial_{t_1}^2 + \partial_{t_2}^2 . \tag{4.38}$$

As a second step, the first order derivatives in t_1 and t_2 are removed by conjugating with

$$\omega(t_1,t_2,w_1,w_2,\Upsilon) = (\sinh t_1 \sinh t_2)^{1-\frac{d}{2}} (\cosh t_1 - \cosh t_2)^{-a-b-\frac{1}{2}} (\cosh t_1 + \cosh t_2)^{a+b-\frac{1}{2}} \left(\frac{\sinh t_1 - \sinh t_2}{\sinh t_1 + \sinh t_2} w_1^2\right)^{\frac{l_a}{2}} \left(\frac{\sinh t_1 + \sinh t_2}{\sinh t_1 - \sinh t_2}(1-w_2)^2\right)^{\frac{l_b}{2}} . \tag{4.39}$$

Finally, we can eliminate all mixed derivatives that involve the t_i coordinates by taking the change of variables

$$\begin{aligned} X_L &= \frac{\sinh t_1 + \sinh t_2}{\sinh t_1 - \sinh t_2}\frac{1-w_1}{w_1} , \qquad X_R = \frac{\sinh t_1 - \sinh t_2}{\sinh t_1 + \sinh t_2}\frac{w_2}{1-w_2} , \\ Y &= -\sqrt{\frac{(1-w_1)w_2}{(1-w_2)w_1}}\frac{\sinh t_1 \sinh t_2}{\cosh t_1 - \cosh t_2}\Upsilon . \end{aligned} \tag{4.40}$$

The operator obtained at the end of this procedure corresponds precisely to the one constructed in subsection 4.2.2.

JHEP06(2022)144

5 Conclusions and outlook

The central goal of this work was to introduce a new set of multipoint cross ratios for correlation functions in higher dimensional CFT that are well adapted to taking OPE limits in the intermediate channels. We achieved this goal for comb channel diagrams of scalar N-point functions in $d = 3, 4$. The strategy we have used here lends itself to several fairly obvious extensions. In particular, given the nice geometrical interpretation of the new cross ratios described in section 3, it seems clear how to extend the construction of cross ratios to higher dimension and a higher number N of insertion points. Recall that every time we increase the dimension d, we obtain one new type of cross ratio, for either vertices or links. Here, the most complicated of such variables to construct was the six-point invariant Υ, which first appears for six-point functions in $d = 4$. Going to $d = 5$, comb channel vertices can carry two variables, starting from $N = 7$. We expect that this new variable is related to the angle between two 4-dimensional subspaces in $d = 5$ dimensions, in a way that preserves all of the nice properties we described above.

We have verified the factorisation of multipoint blocks in the OPE limit only for $N = 6$. Since there are no new types of cross ratios in $d = 4$ as we increase N, we conjecture that our factorisation statement extends to any number of insertion points for comb channel blocks in $d = 4$. It would of course be reassuring to prove this statement. Further in this direction, it would be interesting to study OPE limits and the associated factorisation for higher $N = d + 2 > 6$. Recall from our discussion in section 3.2 that each time we increase d/N, one new polynomial cross ratio appears involving all $d + 2$ insertion points. Given the nice geometric interpretation of our OPE variables for $d \leq 4$ as angles between hyperplanes of increasing dimension, it is tempting generalise the very same construction to higher d. In this way, it is rather straightforward to construct a complete set of variables with a very good chance of being well adapted to OPE limits on intermediate exchange channels with more than three cross ratios. Nonetheless, this should be verified in at least a few more examples. Finally, it would certainly be very rewarding to go beyond the comb channel topology and construct OPE cross ratios for other OPE channels, such as e.g. the snowflake channel.

In this work, we have seen how one can recover lower point blocks of spinning fields from N-point blocks of scalars. In particular, by taking the appropriate OPE limits, it is possible to recover spinning three-point and four-point blocks. Ultimately, it would be important to go in the opposite direction, i.e. to learn how to build multipoint blocks of scalar fields from their three and four-point constituents. Note that the latter are reasonably well understood, while multipoint blocks in dimensions $d > 2$ remain very difficult to evaluate. We have recently made some partial steps in this direction for a two-variable subsystem of scalar five-point blocks, obtained by taking the full OPE limit on one side and a lightcone limit on the other. The resulting system of differential operators, which contains a vertex and the lightcone limit of a Casimir operator, can indeed be solved in terms of the solution of the two subsystems. We plan to return to this and other examples in the near future.

In section 4 of this work, we have made us of some recent progress concerning a universal construction of Casimir operators for spinning four-point blocks. The full derivation of

JHEP06(2022)144

our formulas, along with some other applications of these developments, e.g. to boundary and defect CFT, will be discussed in much more detail in the upcoming paper [43]. The universal construction of the Casimir operators also hints at the existence of a universal power series solutions based on so-called Harish-Chandra coefficients. Replacing these coefficients by concrete representation operators should yield a series expansion for spinning blocks, at least in principle.

Analytic bootstrap constraints on data of higher dimensional conformal field theories from the study of multipoint correlation functions have recently been approached, e.g. through OPE statistics [53], as well as the lightcone bootstrap [51]. In the context of the six-point snowflake channel, the multipoint lightcone bootstrap has begun to produce interesting new insights into the large spin behaviour of three-point couplings involving two and three double twist operators [52]. Similarly, adapting the lightcone bootstrap to six-point functions in the comb channel is expected to provide access to triple trace operators. But for the moment, the relevant comb channel blocks are not well understood, even in the lightcone limit. Using the same methods as in this paper to compute Casimir differential operators in the lightcone limits, we can likely obtain sufficient control over such comb channel lightcone blocks.

Acknowledgments

We are grateful to Gleb Arutyunov, Luke Corcoran, Pavel Etingof, Aleix Gimenez-Grau, Mikhail Isachenkov, Apratim Kaviraj, Madalena Lemos, Pedro Liendo, Nikolai Reshetikhin, Junchen Rong, Evgeny Sobko, Jasper Stokman, Joerg Teschner and Benoît Vicedo for useful discussions. This project received funding from the German Research Foundation DFG under Germany's Excellence Strategy — EXC 2121 Quantum Universe — 390833306 and from the European Union's Horizon 2020 research and innovation programme under the MSC grant agreement No.764850 "SAGEX". S.L. is supported by Dr. Max Rössler, the Walter Haefner Foundation and the ETH Zürich Foundation. I.B. is funded by a research grant under the project H2020 ERC STG 2017 G.A. 758903 "CFT-MAP".

A Euclidean conformal group

Here we spell out our conventions for the conformal group $\mathrm{SO}(d+1,1)$ and its Lie algebra and state some identities valid in the vector representation. The non-vanishing Lie brackets in $\mathfrak{so}(d+1,1)$ read

$$[M_{\mu\nu}, P_\rho] = \delta_{\nu\rho} P_\mu - \delta_{\mu\rho} P_\nu, \qquad [M_{\mu\nu}, K_\rho] = \delta_{\nu\rho} K_\mu - \delta_{\mu\rho} K_\nu, \tag{A.1}$$

$$[M_{\mu\nu}, M_{\rho\sigma}] = \delta_{\nu\rho} M_{\mu\sigma} - \delta_{\mu\rho} M_{\nu\sigma} + \delta_{\nu\sigma} M_{\rho\mu} - \delta_{\mu\sigma} M_{\rho\nu}, \tag{A.2}$$

$$[D, P_\mu] = P_\mu, \qquad [D, K_\mu] = -K_\mu, \qquad [K_\mu, P_\nu] = 2\left(M_{\mu\nu} - \delta_{\mu\nu} D\right). \tag{A.3}$$

Indices μ, ν run from 1 to d. In the Lorentz-like notation, we write the generators as $\{L_{AB}\}$, $A, B = -1, 0, \ldots, d$. These obey the relations

$$[L_{AB}, L_{CD}] = \eta_{BC} L_{AD} - \eta_{AC} L_{BD} + \eta_{BD} L_{CA} - \eta_{AD} L_{CB}, \tag{A.4}$$

JHEP06(2022)144

where $\eta = \text{diag}(-1, 1, \ldots, 1)$. The relation between conformal and Lorentz generators reads

$$L_{-1,0} = D, \qquad L_{-1,\mu} = \frac{1}{2}(P_\mu + K_\mu), \qquad L_{0\mu} = \frac{1}{2}(P_\mu - K_\mu), \qquad L_{\mu\nu} = M_{\mu\nu}\,. \tag{A.5}$$

In the $(d+2)$-dimensional vector representation, the Lorentz generators are

$$L_{AB} = \eta_{AC} E_{CB} - \eta_{BC} E_{CA}, \tag{A.6}$$

where $(E_{AB})_{ij} = \delta_{Ai}\delta_{Bj}$.

A.1 Radial decomposition of the Casimir

The quadratic Casimir $C_2 = -\frac{1}{2} L^{AB} L_{AB}$ can be written as

$$C_2 = L_{-1,0}^2 + L_{-1,1}^2 + L_{-1,2}^2 - L_{01}^2 - L_{02}^2 - L_{12}^2 - L^{-1,a}L_{-1,a} - L^{0a}L_{0a} - L^{1a}L_{1a} - L^{2a}L_{2a} - \frac{1}{2}L^{ab}L_{ab}\,. \tag{A.7}$$

Here, indices a, b take values $3, 4, \ldots, d$. Using relations

$$\begin{aligned} L_{-1,a} &= \coth t_1 M_{1a} - \frac{1}{\sinh t_1} M'_{1a} \\ L_{0a} &= i\left(\coth t_2 M_{2a} - \frac{1}{\sinh t_2} M'_{2a}\right), \end{aligned} \tag{A.8}$$

$$L_{01} \mp i L_{-1,2} = -\coth(t_1 \pm t_2) D_\pm + \frac{D'_\pm}{\sinh(t_1 \pm t_2)}, \tag{A.9}$$

$$\begin{aligned} [M_{1a}, M'_{1a}] &= -\sinh t_1 H_1, \\ [M_{2a}, M'_{2a}] &= -\sinh t_2 H_2, \\ [D_\pm, D'_\pm] &= 2\sinh(t_1 \pm t_2)(H_1 \pm H_2), \end{aligned} \tag{A.10}$$

we obtain

$$-L^{-1,a}L_{-1,a} - L^{1a}L_{1a} = \frac{M'_{1a}M'_{1a} - 2\cosh t_1 M'_{1a}M_{1a} + M_{1a}M_{1a}}{\sinh^2 t_1} + (d-2)\coth t_1 H_1,$$

$$-L^{0a}L_{0a} - L^{2a}L_{2a} = \frac{M'_{2a}M'_{2a} - 2\cosh t_2 M'_{2a}M_{2a} + M_{2a}M_{2a}}{\sinh^2 t_2} + (d-2)\coth t_2 H_2,$$

and

$$\begin{aligned} &L_{-1,0}^2 - L_{12}^2 + L_{-1,2}^2 - L_{01}^2 \\ &= -\frac{D'^2_+ - 2\cosh(t_1+t_2)D'_+D_+ + D^2_+}{2\sinh^2(t_1+t_2)} - \frac{D'^2_- - 2\cosh(t_1-t_2)D'_-D_- + D^2_-}{2\sinh^2(t_1-t_2)} \\ &\quad + \coth(t_1+t_2)(H_1+H_2) + \coth(t_1-t_2)(H_1-H_2)\,. \end{aligned}$$

Adding these terms gives the radial decomposition used in the main text.

JHEP06(2022)144

B Construction of a six-point conformal frame

In this section, we construct a conformal frame for the six-point function by appending x_6 to the conformal frame of the (12345) five-point function, namely:

$$x_1 = \varrho_1 \vec{n}(\theta_1, 0, 0), \quad x_2 = 0, \quad x_3 = \infty, \quad x_4 = \vec{e}_1, \quad x_5 = \vec{e}_1 - \varrho_2 \vec{n}(\theta_2, \phi_1, 0), \tag{B.1}$$

where we parameterise unit vectors in S^4 as

$$\vec{n}(\theta, \phi, \varphi) := \cos\theta\, \vec{e}_1 + \sin\theta \{ \cos\phi\, \vec{e}_2 + \sin\phi\, (\cos\varphi\, \vec{e}_3 + \sin\varphi\, \vec{e}_4) \} = e^{\varphi M_{34}} e^{\phi M_{23}} e^{\theta M_{12}} \vec{e}_1. \tag{B.2}$$

It will also be useful to define the rotation matrices

$$R(\theta, \phi, \varphi) := e^{-\theta M_{12}} e^{-\phi M_{23}} e^{-\varphi M_{31}} \Longrightarrow \vec{n}(\theta, \phi, \varphi) = R(\theta, \phi, \varphi)^{-1} \vec{e}_1. \tag{B.3}$$

Finally, we parameterise cross ratios as in (2.29),

$$z_r := \varrho_r e^{\mathrm{i}\theta_r}, \qquad \bar{z}_r := \varrho_r e^{-\mathrm{i}\theta_r}, \qquad w_s := \sin^2 \frac{\phi_s}{2}, \qquad \Upsilon := \pm \mathrm{i} \frac{\cos\varphi}{\sin\theta_2}. \tag{B.4}$$

To understand how x_6 depends on the cross ratios, we compute a distinguished vector in this frame:

$$\psi_{56} := \left(x_{45}^{-1} - x_{46}^{-1} \right)^{-1} \in \mathbb{R}^4_{1234}, \tag{B.5}$$

where $x^{-1} := x/x^2$ denotes the image of the vector x under conformal inversion. Note that we implicitly used the residual $\mathrm{SO}(d-4)$ symmetry preserving (B.1) to fix a gauge where $x_6 \in \mathrm{Span}(\vec{e}_1, \vec{e}_2, \vec{e}_3, \vec{e}_4)$. In Euclidean signature, we can parameterise the latter by its norm and its unit vector on the S^4, which we write as

$$\psi_{56} = |\psi_{56}|\, \hat{\psi}_{56}, \quad |\psi_{56}| = \varrho_2 \varrho_3^{-1}, \tag{B.6}$$

Then the unit vector $\hat{\psi}_{56}$ is determined by three equations:

$$\hat{\psi}_{56} \cdot \hat{x}_{45} = \frac{1 + u_2 - v_2}{2\varrho_2}, \qquad \hat{\psi}_{56} \cdot x_4 = \frac{\mathcal{U}_2^{(5)}}{2\varrho_2\varrho_3}, \qquad \hat{\psi}_{56} \cdot \hat{x}_1 = \frac{\mathcal{U}_1^{(6)}}{2\varrho_1\varrho_2\varrho_3}, \tag{B.7}$$

where the $\mathcal{U}_r^{(m)}$ are polynomials in the polynomial cross ratios:

$$\mathcal{U}_r^{(5)} := 1 - v_r - v_{r+1} + U_r^{(5)}, \qquad \mathcal{U}_1^{(6)} := (1 - v_1)(1 - v_3) - v_2 + U_1^{(5)} + U_2^{(5)} - U_1^{(6)}. \tag{B.8}$$

Using the change of variables (2.25) and (2.26), we can express the scalar products of (B.7) in terms of the angle cross ratios $(\theta_s, \phi_r, \varphi)$:

$$\frac{\mathcal{U}_1^{(5)}}{2\varrho_2\varrho_3} = \cos\theta_2 \cos\theta_3 + \sin\theta_2 \sin\theta_3 \cos\phi_2 \tag{B.9}$$

$$\begin{aligned} \frac{\mathcal{U}_1^{(6)}}{2\varrho_1\varrho_2\varrho_3} = {} & \cos\theta_1 \cos\theta_2 \cos\theta_3 + \cos\theta_1 \sin\theta_2 \cos\phi_2 \sin\theta_3 + \sin\theta_1 \sin\theta_2 \cos\phi_1 \cos\theta_3 \\ & - \sin\theta_1 \left(\cos\theta_2 \cos\phi_1 \cos\phi_2 + \sin\phi_1 \sin\phi_2 \cos\varphi \right) \sin\theta_3. \end{aligned} \tag{B.10}$$

Given that $x_4 = \vec{e}_1$, $\hat{x}_1 \in \text{Span}(\vec{e}_1, \vec{e}_2)$, $\hat{x}_{45} \in \text{Span}(\vec{e}_1, \vec{e}_2, \vec{e}_3)$, we can recursively compute the components of $\hat{\psi}_{56}$ as

$$\begin{aligned}
\hat{\psi}_{56} \cdot x_4 = \hat{\psi}_{56} \cdot \vec{e}_1 &\Longrightarrow \hat{\psi}^1_{56}, \\
\hat{\psi}_{56} \cdot \hat{x}_1 = \hat{\psi}_{56} \cdot \vec{n}(\theta_1, 0, 0) &\Longrightarrow \hat{\psi}^2_{56}, \\
\hat{\psi}_{56} \cdot \hat{x}_{45} = \hat{\psi}_{56} \cdot \vec{n}(\theta_2, \phi_1, 0) &\Longrightarrow \pm\hat{\psi}^3_{56}, \\
(\hat{\psi}^1_{56})^2 + (\hat{\psi}^2_{56})^2 + (\hat{\psi}^3_{56})^2 + (\hat{\psi}^4_{56})^2 = 1 &\Longrightarrow \pm\hat{\psi}^4_{56}.
\end{aligned}$$

There is a sign indeterminacy in the third step coming from the convention for $\Upsilon \propto \pm\cos\varphi$, and there is also a sign indeterminacy in the last step coming from the two solutions to the quadratic equation. We compute the solution to each of these equations and find

$$\hat{\psi}_{56} = R(\theta_2, \phi_1, 0)^{-1}\vec{n}(-\theta_3, \pm\phi_2, \pm\varphi) \overset{\text{choice}}{=} R(\theta_2, \phi_1, 0)^{-1}\vec{n}(-\theta_3, \phi_2, \varphi). \tag{B.11}$$

Now, we can obtain x_6 in the conformal frame by a conformal transformation of ψ_{56},

$$\psi_{56} = (x_{64}^{-1} - x_{54}^{-1})^{-1} = e^{-x_{45}^{-1}\cdot K} e^{x_4 \cdot P} \cdot x_6 = e^{-\varrho_2^{-1}\vec{n}(\theta_2,\phi_1,0)\cdot K} e^{P_1} x_6. \tag{B.12}$$

After simplifying and inverting the conformal transformation in (B.12), we then obtain

$$x_6 = e^{-P_1}\varrho_2^{-D} R(\theta_2, \phi_1, 0)^{-1}\mathcal{I}\, e^{P_1} \cdot \varrho_3 n(-\theta_3, \phi_2, \varphi), \tag{B.13}$$

where $\mathcal{I} : x \mapsto x^{-1}$ is conformal inversion. To better understand the meaning of these conformal transformations, let's take a closer look at the conformal group element

$$g \equiv g(\varrho_2, \theta_2, \phi_1) = e^{-P_1}\varrho_2^{-D} R(\theta_2, \phi_1, 0)^{-1}\mathcal{I}\, e^{P_1}. \tag{B.14}$$

Its inverse acts as

$$g^{-1} : x \mapsto \varrho_2^{-1} R(\theta_2, \phi_1)(x - \vec{e}_1)^{-1} + \vec{e}_1, \tag{B.15}$$

such that when g^{-1} acts on the points of the original conformal frame, the images are given by

$$g^{-1}(x_6) = \varrho_3\vec{n}(-\theta_3, \phi_2, \varphi), \qquad g^{-1}(x_5) = 0, \qquad g^{-1}(x_4) = \infty, \qquad g^{-1}(x_3) = \vec{e}_1. \tag{B.16}$$

This suggests a general method to characterise the comb channel conformal frame of $N > 6$ points in $d = 4$, which depends on the cross ratios $(\varrho_r, \theta_r)_{r=1}^{N-3}$, $(\phi_s)_{s=1}^{N-4}$ and $(\varphi_r)_{r=2}^{N-4}$ defined in (2.35). First, define the conformal transformation

$$h^{-1}(\varrho_2, \theta_2, \phi_1, 0, \varphi_2) := e^{-\varphi_2 M_{34}}\sigma_1\, e^{P_1} g^{-1}(\varrho_2, \theta_2, \phi_1) = \varrho_2^{-D}\mathcal{I}\sigma_1 e^{-\varphi_2 M_{zt}} R(\theta_2, \phi_1) e^{P_1}, \tag{B.17}$$

where $\sigma_1 : (x^1, x^2, x^3, x^4) \mapsto (-x^1, x^2, x^3, x^4)$ is a reflection along the hyperplane orthogonal to $\vec{e}_1$. Its action on a point is given by

$$h^{-1}(x) = \varrho_2\sigma_1 e^{-\varphi_2 M_{34}} R(\theta_2, \phi_1)(x - \vec{e}_1)^{-1}. \tag{B.18}$$

From the previous discussion, we determined that this conformal transformation acts on the six-point conformal frame as follows:

$$\begin{aligned} &h^{-1}(x_2) = \varrho_2\vec{n}(\theta_2,0,0), && h^{-1}(x_3) = 0, && h^{-1}(x_4) = \infty, \\ &h^{-1}(x_5) = \vec{e}_1, && h^{-1}(x_6) = \vec{e}_1 - \varrho_3\vec{n}(\theta_3,\phi_2,0). \end{aligned} \tag{B.19}$$

Thus, h^{-1} shifts the framing from the constraints (B.1) on x_i, to the same constraints on x_{i+1}, $i = 1,\ldots,5$. We can similarly express the seventh point as

$$h^{-1}(x_7) = h'\left(\vec{e}_1 - \varrho_4\vec{n}\left(\theta_4,\phi_3,0\right)\right), \tag{B.20}$$

where $h' \equiv h(\varrho_3,\theta_3,\phi_2,\varphi_2,\varphi_3)$ is now uniquely defined by

$$\begin{aligned} &h'^{-1}(0) = \varrho_3\vec{n}(\theta_3,0,0), && h'^{-1}(\infty) = 0, && h'^{-1}(e_x) = \infty, \\ &h'^{-1}(h^{-1}(x_6)) = \vec{e}_1, && h'^{-1}(h^{-1}(x_7)) = \vec{e}_1 - \varrho_4\vec{n}(\theta_4,\phi_3,0). \end{aligned}$$

A quick comparison with the action of h^{-1} on $x_2,\ldots,x_6$ implies that

$$h'^{-1} := \varrho_3^{-D}\mathcal{I}\sigma_1 e^{-\varphi_3 M_{34}} R(\theta_3,\phi_2,\varphi_2)^{-1} e^{P_1}. \tag{B.21}$$

We can then iterate this procedure until reaching x_N. More specifically, the frame will be given by

$$\begin{aligned} x_1 &= \varrho_1\vec{n}\left(\theta_1,0,0\right), \\ x_2 &= 0, \\ x_3 &= \infty, \\ x_4 &= \vec{e}_1, \\ x_5 &= \vec{e}_1 - \varrho_2\vec{n}\left(\theta_2,\phi_1,0\right), \\ x_6 &= h\left(\varrho_2,\theta_2,\phi_1,\varphi_1,0\right)\left(\vec{e}_1 - \varrho_3\vec{n}\left(\theta_3,\phi_2,0\right)\right) \\ x_7 &= h\left(\varrho_2,\theta_2,\phi_1,\varphi_1,0\right)\circ h\left(\varrho_3,\theta_3,\phi_2,\varphi_1,\varphi_2\right)\left(\vec{e}_1 - \varrho_4\vec{n}\left(\theta_4,\phi_3,0\right)\right), \\ &\cdots\cdots\cdots \\ x_N &= h\left(\varrho_2,\theta_2,\phi_1,\varphi_1,0\right)\circ\prod_{r=3}^{N-4} h\left(\varrho_r,\theta_r,\phi_{r-1},\varphi_{r-1},\varphi_r\right)\left(\vec{e}_1 - \varrho_N\vec{n}\left(\theta_N,\phi_{N-1},\varphi_{N-2},0\right)\right), \end{aligned}$$

where

$$h^{-1}(\varrho_r,\theta_r,\phi_{r-1},\varphi_{r-1},\varphi_r) := \varrho_r^{-D}\mathcal{I}\sigma_1 e^{-\varphi_r M_{34}} R(\theta_r,\phi_{r-1},\varphi_{r-1})^{-1} e^{P_1}. \tag{B.22}$$

The action of this conformal group element on points is then given by

$$h^{-1}(\varrho_r,\theta_r,\phi_{r-1},\varphi_{r-1},\varphi_r) : x \mapsto \varrho_r\sigma_1 e^{-\varphi_r M_{34}} R(\theta_r,\phi_{r-1},\varphi_{r-1})^{-1}(x-\vec{e}_1)^{-1}. \tag{B.23}$$

C Middle leg OPE limit in embedding space

In the six-point function, the limit $\bar{z}_2 \to 0$ at the middle leg b can be lifted to embedding space as

$$X_{45}, X_{46}, X_{56} \to 0, \qquad \frac{X_{45}}{X_{46}}, \frac{X_{56}}{X_{46}} = \text{finite}. \tag{C.1}$$

In other words, all distances between the three points x_4, x_5 and x_6 vanish at the same rate in spacetime. By first quantising around x_6 and then mapping to the cylinder, a triplet satisfying (C.1) is mapped to past timelike infinity. The infinite distance between (x_4, x_5, x_6) and (x_1, x_2, x_3) in this limit factorises the six-point function into a product of two four-point functions, in a manner reminiscent of the cluster decomposition principle.

To compute this limit in embedding space, it will be useful to define the vector

$$Y_5 := (X_4 - X_5) - \frac{X_{45}}{X_{46}} (X_4 - X_6) . \tag{C.2}$$

In particular, $X_4 \wedge Y_5$ is a homogeneous tensor in both X_4 and X_5. For a spacetime interpretation of this vectors, recall the reduction $X, Z \mapsto x, z$ of a STT to the Poincare patch:

$$X_x = \left(\frac{1+x^2}{2}, \frac{1-x^2}{2}, x \right) , \qquad Z_{x,z} = (x \cdot z, -x \cdot z, z). \tag{C.3}$$

If we put all embedding space vectors in this patch, $X_i := X_{x_i}$, we obtain

$$Y_5 = \frac{x_{56}^2}{x_{46}^2} Z_{x_4, \psi_{56}}, \qquad \psi_{56} := \left(x_{45}^{-1} - x_{46}^{-1} \right)^{-1} . \tag{C.4}$$

Note also that $Y_5^2 = -2 \frac{X_{45} X_{56}}{X_{46}} \to 0$ in the limit (C.1). We now define the full b OPE limit $z_2, \Upsilon \to 0$ in embedding space as

$$X_5 = X_4 + \epsilon Z_4, \qquad Y_5 = \epsilon \epsilon' W_4, \qquad \epsilon, \epsilon' \to 0. \tag{C.5}$$

where Z_4 and W_4 are MST_2 polarisation vectors for X_4. To make the connection with the prescription of section 3.2 more explicit, we can rewrite the second equation in (C.5) as

$$\epsilon' W_4 = Z_4' - Z_4, \qquad \epsilon Z_4' := \frac{X_{45}}{X_{46}} (X_6 - X_4). \tag{C.6}$$

We thereby obtain the same prescription as eq. (3.19) up to projective equivalence, with a rescaling of Z_4' outside of the conventional Poincare patch to simplify computations. Note that the permutation $(4, 5, 6) \leftrightarrow (3, 2, 1)$ leads to an identical parameterisation of the b OPE limit. Thus, to make expressions more symmetric, we also define

$$Y_2 := Y_5|_{(4,5,6) \leftrightarrow (3,2,1)}. \tag{C.7}$$

Now, to understand how Υ encodes MST_2 transfer along the internal leg b, we would like to compute the b OPE limit of

$$\frac{X_{34} (X_3 \wedge X_2 \wedge Y_2) \cdot (X_4 \wedge X_5 \wedge Y_5)}{X_{24}^2 X_{35}^2} = \mathcal{U}_1^{(5)} \mathcal{U}_2^{(5)} - (1 - v_2) \mathcal{U}_1^{(6)}, \tag{C.8}$$

where $\mathcal{U}_r^{(m)}$ are the same functions of the polynomial cross-ratios defined in (B.8). To relate them to the left hand side of (C.8), we expressed them in embedding space as follows:

$$\mathcal{U}_1^{(5)} = \frac{(X_3 \wedge Y_2)\cdot(X_4 \wedge X_5)}{X_{24}X_{35}}, \qquad \mathcal{U}_2^{(5)} = \frac{(X_3 \wedge X_2)\cdot(X_4 \wedge Y_5)}{X_{24}X_{35}},$$
$$\mathcal{U}_1^{(6)} = \frac{(X_3 \wedge Y_2)\cdot(X_4 \wedge Y_5)}{X_{24}X_{35}}. \tag{C.9}$$

On the left hand side of (C.8), the OPE limit (C.5) is simple to compute:

$$\text{LHS} = \epsilon^2\epsilon' \frac{X_{23}U_{4,123}}{X_{13}X_{24}^2X_{34}} + \mathcal{O}\left(\epsilon^3\epsilon'\right), \qquad U_{4,123} := (X_4 \wedge Z_4 \wedge W_4)_{ABC}\, X_1^A X_2^B X_3^C.$$

Note that $U_{4,123}$ is the unique independent MST_2 tensor structure of the four-point function of three scalars and one MST_2 field. On the other hand, the right hand side of (C.8) can be written in cross ratio space using

$$\mathcal{U}_1^{(5)} = z_1' z_2 + \bar{z}_1' \bar{z}_2, \tag{C.10}$$

$$\mathcal{U}_2^{(5)} = z_2 z_3' + \bar{z}_2 \bar{z}_3', \tag{C.11}$$

$$\mathcal{U}_1^{(6)} = z_1' z_2 z_3' + \bar{z}_1' \bar{z}_2 \bar{z}_3' - \left[(z_1 - \bar{z}_1)\sqrt{w_1(1-w_1)}\right](z_2 - \bar{z}_2)\Upsilon\left[(z_3 - \bar{z}_3)\sqrt{w_2(1-w_2)}\right], \tag{C.12}$$

where we defined

$$z_1' := w_1 z_1 + (1-w_1)\bar{z}_1, \qquad \bar{z}_1' := w_1 \bar{z}_1 + (1-w_1) z_1, \tag{C.13}$$

$$z_3' := w_2 z_3 + (1-w_2)\bar{z}_3, \qquad \bar{z}_3' := w_2 \bar{z}_3 + (1-w_2) z_3. \tag{C.14}$$

Taking $\bar{z}_2 = 0$, we then find

$$\mathcal{U}_1^{(5)}\mathcal{U}_2^{(5)} - (1-v_2)\mathcal{U}_1^{(6)} = \frac{1}{4}\left[(z_1 - \bar{z}_1)\sqrt{w_1(1-w_1)}\right] z_2^2 \Upsilon \left[(z_3 - \bar{z}_3)\sqrt{w_2(1-w_2)}\right]. \tag{C.15}$$

At the same time, using

$$1 - v_2 = z_2 = \epsilon \frac{J_{4,23}}{X_{24}X_{34}} + \mathcal{O}\left(\epsilon^2\right), \qquad J_{4,23} := (X_4 \wedge Z_4)_{BC}\, X_2^B X_3^C, \tag{C.16}$$

we find that $\Upsilon = \mathcal{O}(\epsilon')$ in the b OPE limit (C.5) with leading behaviour

$$\Upsilon = \epsilon' \frac{U_{4,123}X_{23}X_{34}}{X_{13}J_{4,23}^2}\left[\frac{z_1 - \bar{z}_1}{2}\frac{z_3 - \bar{z}_3}{2}\sqrt{w_1(1-w_1)}\sqrt{w_2(1-w_2)}\right]^{-1} + \mathcal{O}\left(\epsilon\epsilon'\right). \tag{C.17}$$

In particular, if we define

$$\deg X_4^{-\Delta} Z_4^l W_4^\ell := [\Delta, l, \ell] \Longrightarrow \deg J_{4,23} = [-1,1,0], \qquad \deg U_{4,123} = [-1,1,1], \tag{C.18}$$

then we find from (C.16) and (C.17) that

$$\deg z_2 = [1,1,0], \qquad \deg \bar{z}_2 = [1,-1,0], \qquad \deg \Upsilon = [0,-1,1]. \tag{C.19}$$

This fits directly with the asymptotic behaviour (3.28) of conformal blocks in the b OPE limit.

JHEP06(2022)144

D OPE limit factorisation of six-point blocks in one-dimensional CFT

Let us consider the case of six-point conformal blocks in the comb channel for the $d = 1$ case. In this case, the conformal blocks have already been computed in [15]. To match the conventions of that paper, we introduce the three cross ratios

$$\chi_1 = \frac{x_{12}x_{34}}{x_{13}x_{24}}\,, \qquad \chi_2 = \frac{x_{23}x_{45}}{x_{24}x_{35}}\,, \qquad \chi_3 = \frac{x_{34}x_{56}}{x_{35}x_{46}}\,, \tag{D.1}$$

which make a complete set of independent cross ratios in $d = 1$, and we rename conformal dimensions as

$$\Delta_i = h_i\,, \qquad \Delta_a = \mathbb{h}_1\,, \qquad \Delta_b = \mathbb{h}_2\,, \qquad \Delta_c = \mathbb{h}_3\,. \tag{D.2}$$

Note that when reducing to $d = 1$, the Gram determinant relations impose $z_i = \bar{z}_i$, and that

$$\chi_i = z_i = \bar{z}_i\,. \tag{D.3}$$

The one-dimensional six-point conformal blocks can then be written as in [15, equation 2.11],

$$g^{h_1,\ldots,h_6}_{\mathbb{h}_1,\mathbb{h}_2,\mathbb{h}_3} = \chi_1^{\mathbb{h}_1}\chi_2^{\mathbb{h}_2}\chi_3^{\mathbb{h}_3} F_K\left[\begin{matrix} h_{12}+\mathbb{h}_1,\ \mathbb{h}_1+\mathbb{h}_2-h_3,\ \mathbb{h}_2+\mathbb{h}_3-h_4,\ \mathbb{h}_3+h_{65} \\ 2\mathbb{h}_1,\ 2\mathbb{h}_2,\ 2\mathbb{h}_3 \end{matrix};\chi_1,\chi_2,\chi_3\right], \tag{D.4}$$

where the comb function F_K can be expressed as

$$F_K\left[\begin{matrix} a_1, b_1, b_2, a_2 \\ c_1, c_2, c_3 \end{matrix};\chi_1,\chi_2,\chi_3\right] = \sum_{n=0}^{\infty} \frac{(b_1)_n (b_2)_n}{(c_2)_n}\frac{\chi_2^n}{n!}\,{}_2F_1\left[\begin{matrix} b_1+n,\ a_1 \\ c_1 \end{matrix};\chi_1\right]{}_2F_1\left[\begin{matrix} b_2+n,\ a_2 \\ c_3 \end{matrix};\chi_3\right]. \tag{D.5}$$

It is immediate to see that the leading behaviour with respect to the cross ratio χ_2, which is the one-dimensional analogue of $\bar{z}_2$, corresponds simply to $n = 0$ in eq. (D.5), leading to the factorised expression

$$\begin{aligned} &g^{h_1,\ldots,h_6}_{\mathbb{h}_1,\mathbb{h}_2,\mathbb{h}_3} \\ &\overset{\chi_2\to 0}{\sim} \chi_2^{\mathbb{h}_2}\left(\chi_1^{\mathbb{h}_1}\,{}_2F_1\left[\begin{matrix} \mathbb{h}_1+\mathbb{h}_2-h_3,\ h_{12}+\mathbb{h}_1 \\ 2\mathbb{h}_1 \end{matrix};\chi_1\right]\right)\left(\chi_3^{\mathbb{h}_3}\,{}_2F_1\left[\begin{matrix} \mathbb{h}_2+\mathbb{h}_3-h_4,\ \mathbb{h}_3+h_{65} \\ 2\mathbb{h}_3 \end{matrix};\chi_3\right]\right). \end{aligned} \tag{D.6}$$

Expression (D.6) is an explicit factorisation of six-point conformal blocks into the product of two four-point blocks, providing an explicit example of equation (3.28) for the one-dimensional case.

JHEP06(2022)144

References

[1] F.A. Dolan and H. Osborn, *Conformal four point functions and the operator product expansion*, *Nucl. Phys. B* **599** (2001) 459 [hep-th/0011040] [INSPIRE].

[2] F.A. Dolan and H. Osborn, *Conformal partial waves and the operator product expansion*, *Nucl. Phys. B* **678** (2004) 491 [hep-th/0309180] [INSPIRE].

[3] F.A. Dolan and H. Osborn, *Conformal Partial Waves: Further Mathematical Results*, arXiv:1108.6194 [INSPIRE].

[4] M.S. Costa, J. Penedones, D. Poland and S. Rychkov, *Spinning Conformal Blocks*, *JHEP* **11** (2011) 154 [arXiv:1109.6321] [INSPIRE].

[5] D. Simmons-Duffin, *Projectors, Shadows, and Conformal Blocks*, *JHEP* **04** (2014) 146 [arXiv:1204.3894] [INSPIRE].

[6] M. Hogervorst and S. Rychkov, *Radial Coordinates for Conformal Blocks*, *Phys. Rev. D* **87** (2013) 106004 [arXiv:1303.1111] [INSPIRE].

[7] J. Penedones, E. Trevisani and M. Yamazaki, *Recursion Relations for Conformal Blocks*, *JHEP* **09** (2016) 070 [arXiv:1509.00428] [INSPIRE].

[8] A. Castedo Echeverri, E. Elkhidir, D. Karateev and M. Serone, *Deconstructing Conformal Blocks in 4D CFT*, *JHEP* **08** (2015) 101 [arXiv:1505.03750] [INSPIRE].

[9] A. Castedo Echeverri, E. Elkhidir, D. Karateev and M. Serone, *Seed Conformal Blocks in 4D CFT*, *JHEP* **02** (2016) 183 [arXiv:1601.05325] [INSPIRE].

[10] M.S. Costa, T. Hansen, J. Penedones and E. Trevisani, *Projectors and seed conformal blocks for traceless mixed-symmetry tensors*, *JHEP* **07** (2016) 018 [arXiv:1603.05551] [INSPIRE].

[11] M. Isachenkov and V. Schomerus, *Integrability of conformal blocks. Part I. Calogero-Sutherland scattering theory*, *JHEP* **07** (2018) 180 [arXiv:1711.06609] [INSPIRE].

[12] D. Karateev, P. Kravchuk and D. Simmons-Duffin, *Weight Shifting Operators and Conformal Blocks*, *JHEP* **02** (2018) 081 [arXiv:1706.07813] [INSPIRE].

[13] R.S. Erramilli, L.V. Iliesiu and P. Kravchuk, *Recursion relation for general 3d blocks*, *JHEP* **12** (2019) 116 [arXiv:1907.11247] [INSPIRE].

[14] J.-F. Fortin, W.-J. Ma, V. Prilepina and W. Skiba, *Efficient rules for all conformal blocks*, *JHEP* **11** (2021) 052 [arXiv:2002.09007] [INSPIRE].

[15] V. Rosenhaus, *Multipoint Conformal Blocks in the Comb Channel*, *JHEP* **02** (2019) 142 [arXiv:1810.03244] [INSPIRE].

[16] S. Parikh, *Holographic dual of the five-point conformal block*, *JHEP* **05** (2019) 051 [arXiv:1901.01267] [INSPIRE].

[17] J.-F. Fortin and W. Skiba, *New methods for conformal correlation functions*, *JHEP* **06** (2020) 028 [arXiv:1905.00434] [INSPIRE].

[18] S. Parikh, *A multipoint conformal block chain in d dimensions*, *JHEP* **05** (2020) 120 [arXiv:1911.09190] [INSPIRE].

[19] J.-F. Fortin, W. Ma and W. Skiba, *Higher-Point Conformal Blocks in the Comb Channel*, *JHEP* **07** (2020) 213 [arXiv:1911.11046] [INSPIRE].

[20] N. Irges, F. Koutroulis and D. Theofilopoulos, *The conformal N-point scalar correlator in coordinate space*, arXiv:2001.07171 [INSPIRE].

JHEP06(2022)144

[21] J.-F. Fortin, W.-J. Ma and W. Skiba, *Six-point conformal blocks in the snowflake channel*, *JHEP* **11** (2020) 147 [arXiv:2004.02824] [INSPIRE].

[22] A. Pal and K. Ray, *Conformal Correlation functions in four dimensions from Quaternionic Lauricella system*, *Nucl. Phys. B* **968 (2021) 115433** [arXiv:2005.12523].

[23] J.-F. Fortin, W.-J. Ma and W. Skiba, *Seven-point conformal blocks in the extended snowflake channel and beyond*, *Phys. Rev. D* **102** (2020) 125007 [arXiv:2006.13964] [INSPIRE].

[24] S. Hoback and S. Parikh, *Towards Feynman rules for conformal blocks*, *JHEP* **01** (2021) 005 [arXiv:2006.14736] [INSPIRE].

[25] V. Gonçalves, R. Pereira and X. Zhou, $20'$ *Five-Point Function from* $AdS_5 \times S^5$ *Supergravity*, *JHEP* **10** (2019) 247 [arXiv:1906.05305] [INSPIRE].

[26] I. Buric, S. Lacroix, J.A. Mann, L. Quintavalle and V. Schomerus, *From Gaudin Integrable Models to d-dimensional Multipoint Conformal Blocks*, *Phys. Rev. Lett.* **126** (2021) 021602 [arXiv:2009.11882] [INSPIRE].

[27] T. Anous and F.M. Haehl, *On the Virasoro six-point identity block and chaos*, *JHEP* **08** (2020) 002 [arXiv:2005.06440] [INSPIRE].

[28] J.-F. Fortin, W.-J. Ma and W. Skiba, *All Global One- and Two-Dimensional Higher-Point Conformal Blocks*, arXiv:2009.07674 [INSPIRE].

[29] I. Buric, S. Lacroix, J.A. Mann, L. Quintavalle and V. Schomerus, *Gaudin models and multipoint conformal blocks: general theory*, *JHEP* **10** (2021) 139 [arXiv:2105.00021] [INSPIRE].

[30] D. Poland and V. Prilepina, *Recursion relations for 5-point conformal blocks*, *JHEP* **10** (2021) 160 [arXiv:2103.12092] [INSPIRE].

[31] M. Gaudin, *Diagonalisation d'une classe d'hamiltoniens de spin*, *J. Phys. (France)* **37** (1976) 1087.

[32] M. Gaudin, *La fonction d'onde de Bethe*, Masson, France (1983) [ISBN: 9782225796074].

[33] B. Feigin, E. Frenkel and N. Reshetikhin, *Gaudin model, Bethe ansatz and correlation functions at the critical level*, *Commun. Math. Phys.* **166** (1994) 27 [hep-th/9402022] [INSPIRE].

[34] I. Buric, S. Lacroix, J.A. Mann, L. Quintavalle and V. Schomerus, *Gaudin models and multipoint conformal blocks. Part II. Comb channel vertices in 3D and 4D*, *JHEP* **11** (2021) 182 [arXiv:2108.00023] [INSPIRE].

[35] P. Etingof, G. Felder, X. Ma and A. Veselov, *On elliptic Calogero-Moser systems for complex crystallographic reflection groups*, *J. Algebra* **329** (2011) 107 [*Erratum*: http://www-math.mit.edu/~etingof/errorsinpapers.pdf] [arXiv:1003.4689].

[36] M. Isachenkov and V. Schomerus, *Superintegrability of d-dimensional Conformal Blocks*, *Phys. Rev. Lett.* **117** (2016) 071602 [arXiv:1602.01858] [INSPIRE].

[37] G.J. Heckman and E.M. Opdam, *Root systems and hypergeometric functions. I*, *Compos. Math.* **64** (1987) 329.

[38] M.S. Costa, J. Penedones, D. Poland and S. Rychkov, *Spinning Conformal Correlators*, *JHEP* **11** (2011) 071 [arXiv:1107.3554] [INSPIRE].

[39] V. Schomerus, E. Sobko and M. Isachenkov, *Harmony of Spinning Conformal Blocks*, *JHEP* **03** (2017) 085 [arXiv:1612.02479] [INSPIRE].

JHEP06(2022)144

[40] V. Schomerus and E. Sobko, *From Spinning Conformal Blocks to Matrix Calogero-Sutherland Models*, *JHEP* **04** (2018) 052 [arXiv:1711.02022] [INSPIRE].

[41] I. Burić, M. Isachenkov and V. Schomerus, *Conformal Group Theory of Tensor Structures*, *JHEP* **10** (2020) 004 [arXiv:1910.08099] [INSPIRE].

[42] Harish-Chandra, *Spherical Functions on a Semisimple Lie Group, I*, *Amer. J. Math.* **80** (1958) 241.

[43] I. Buric and V. Schomerus, *Universal Spinning Casimir Equations. Applications to Defect CFTs*, in preparation.

[44] T.G. Raben and C.-I. Tan, *Minkowski conformal blocks and the Regge limit for Sachdev-Ye-Kitaev-like models*, *Phys. Rev. D* **98** (2018) 086009 [arXiv:1801.04208] [INSPIRE].

[45] L. Iliesiu, F. Kos, D. Poland, S.S. Pufu, D. Simmons-Duffin and R. Yacoby, *Fermion-Scalar Conformal Blocks*, *JHEP* **04** (2016) 074 [arXiv:1511.01497] [INSPIRE].

[46] I. Buric, V. Schomerus and E. Sobko, *Superconformal Blocks: General Theory*, *JHEP* **01** (2020) 159 [arXiv:1904.04852] [INSPIRE].

[47] I. Burić, V. Schomerus and E. Sobko, *The superconformal X-ing equation*, *JHEP* **10** (2020) 147 [arXiv:2005.13547] [INSPIRE].

[48] J. Stokman and N. Reshetikhin, *N-point spherical functions and asymptotic boundary KZB equations*, *Invent. Math.* **229** (2022) 1 [arXiv:2002.02251] [INSPIRE].

[49] N. Reshetikhin and J. Stokman, *Asymptotic boundary KZB operators and quantum Calogero-Moser spin chains*, arXiv:2012.13497 [INSPIRE].

[50] I.O. Burić, *Harmonic Analysis in Conformal and Superconformal Field Theory*, Ph.D. Thesis, Hamburg University, Hamburg, Germany (2021) [DOI].

[51] C. Bercini, V. Gonçalves and P. Vieira, *Light-Cone Bootstrap of Higher Point Functions and Wilson Loop Duality*, *Phys. Rev. Lett.* **126** (2021) 121603 [arXiv:2008.10407] [INSPIRE].

[52] A. Antunes, M.S. Costa, V. Goncalves and J.V. Boas, *Lightcone bootstrap at higher points*, *JHEP* **03** (2022) 139 [arXiv:2111.05453] [INSPIRE].

[53] T. Anous, A. Belin, J. de Boer and D. Liska, *OPE statistics from higher-point crossing*, arXiv:2112.09143 [INSPIRE].

JHEP06(2022)144